# Studies on seasonal re-translocation of phosphorus in deciduous woody plant; Populus alba

栗田, 悠子

(Degree)
博士（理学）

(Date of Degree)
2016-03-25

(Date of Publication)
2018-03-25

(Resource Type)
doctoral thesis

(Report Number)
甲第6610号

(URL)
https://hdl.handle.net/20.500.14094/D1006610

**Contents**

**Abbreviations**

$IP_6$ : myo-inositol-1,2,3,4,5,6-hexakis phosphate: phytic acid

Pi : inorganic phosphate

Po : organic phosphate

EDX : energy dispersive X-ray spectrometry analysis

RRIS : real-time radioisotope imaging system

MAR : microautoradiography

IP : imaging plate

**Summary**

Seasonal efficient use of nutrients is one of the important strategies for perennial plants to enable their long-lasting survival. In the temperate zone, leaves of deciduous perennial plants shed once a year to cope with winter which is unsuitable period for growth, and go into dormancy. In the next spring, dormancy is broken, and after bud burst, the new leaves begin to grow again. The leaf is the photosynthetic apparatus which produces energy for whole plant. In growing season, a large part of the nutrients is concentrated in the leaves. To save these nutrients, deciduous plants remobilize various nutrients (nitrogen, phosphorus, sulfur, etc.) from leaves before leaf fall. Remobilized nutrients are stored in perennial tissues (twigs, buds, stem, roots) during winter, and in the next spring, re-used for the new growth.

The seasonal use of nutrients, re-translocation from source to sink tissues, storage during dormancy, re-use in new growing season, environmental cues and their regulation mechanisms have been investigated mainly about carbon (C) and nitrogen (N). On the other hand, as for phosphorus (P), although there are some reports about the remobilization from senescing leaves in autumn, there are few reports about other seasonal events of P recycle in perennial plants.

Phosphorus is an essential element for plant growth and development, but its supply from the soil is often limited in natural and agricultural environments. Plants employ multiple physiological strategies to minimize the negative impact of phosphate deficiency. Physiological and molecular strategies about P acquisition, recycling and/or maintenance P homeostasis have been intensively investigated with annual herbaceous plants, like *Arabidopsis thaliana*. In deciduous perennial plants, little is known about seasonal P recycling, storage and mobilization. The tissue where the P is stored and the molecular form of storage during the winter have not been clarified. It is also unknown

how tree controls the seasonal re-translocation and distribution of the phosphorus in tissues.

To resolve these questions, the following investigations were conducted using a deciduous woody plant, *Populus alba* L.

## ■ Chapter 1 Annual re-translocation and storage of phosphate in field-growing poplar trees

To clarify seasonal distribution of phosphate and molecular form during winter, inorganic and organic phosphates were measured in leaves and twigs in the deciduous woody plant, *Populus alba*. The annual changes in leaf phosphate contents of white poplar (*Populus alba*) growing under natural conditions revealed that about 75 % of inorganic and 60 % of organic leaf phosphates contained in May were remobilized by November. In poplar twigs, inorganic phosphate was abundant in growing season, then decreased from summer to winter. On the other hand, organic phosphates were highly accumulated in twigs from late summer to winter, and $IP_6$ (myo-inositol-1,2,3,4,5,6-hexakis phosphate: phytic acid) showed the seasonal pattern similar to winter storage of the organic phosphates. $IP_6$ was largely accumulated in winter twigs and almost disappeared in early spring. The electron microscopic observations showed that, in protein storage vacuoles of parenchyma cells of the winter twig, phosphorus localized at electron-dense structures like globoids known as phosphorus reserver in angiosperm plants' seeds. These findings suggest that $IP_6$ is the seasonal phosphorus reservoir in the deciduous woody plant, *Populus alba*.

## ■ Chapter 2 Establishment of a shortened annual cycle system in laboratory

It has been known that seasonal events, like growth cessation, autumn senescence and bud break, are under the control of photoperiod and temperature. In order to analyze the process of seasonal re-translocation of phosphorus, a model system,

which can be simulated annual cycle of phosphate re-translocation in trees under laboratory condition was established by controlling temperature and photoperiod. This model system was named “shortened annual cycle”. This system has three independent environmental conditions, stage 1 is “a growing season like spring and summer”, stage 2 is “an autumn for adaptation to winter” and stage 3 is “a setting period for winter dormancy and dormancy break”. In stage 2, plants are exposed to short day photoperiod and moderate temperature to induce growth cessation and subsequent autumn senescence. In stage 3, plants are exposed to severer low temperature to be accelerated autumn senescence and undergone chilling for dormancy release. After leaf fall, when plants are moved to the stage 1, bud break is induced. This shortened annual cycle system in laboratory condition evidently allowed us to monitor the annual changes in leaf color, phosphate remobilization from senescent leaves, organic phosphate and $IP_6$ accumulation in the stem during dormancy, and bud break in the next spring within five months. We can always obtain experimental materials, which are in the different season by this system.

## ■ Chapter 3 Analysis of seasonal re-translocation of phosphorus by autoradiography

Changes in seasonal P distribution in poplar trees were evident (chapter 1), and it was suggested that P re-translocation from old leaves to young leaves (chapter 2) and P remobilization from senescing leaves to twig (stem) occur in autumn and winter. Although it was known that P was re-translocated from source tissues to sink tissues mainly via phloem in herbaceous plants, seasonal re-translocation route in deciduous trees is unknown. To investigate how poplar trees re-translocate P from source tissues to sink tissues, seasonal re-translocation and accumulation of phosphorus were analyzed by using autoradiography of trees under the shortened annual cycle system. From stage

1 to stage 3, the transition of phosphate sink tissues was observed. In stage 1, shoot apex and young leaves were main sink tissues. By phloem girdling, it was confirmed that re-translocation of phosphate occurred mainly via phloem. Phosphate appeared to be re-translocated toward both the upward and the downward directions. On the other hand, slow re-translocation via xylem toward the upward direction was also observed. This indicates existence of phloem-xylem exchange of P. In stage 3, remobilized phosphate was mainly accumulated in the stem. At cellular level in the stem, phosphorus remobilized from a leaf was mainly detected in phloem in stage 1. In stage 3, phosphorus was detected in phloem, cortex, ray, and perimedullary zone. These results suggest that phosphate is re-translocated via phloem and storage ability in the stem is activated during senescing period. Furthermore, phosphate stored in the stem in stage 3 was detected in new shoots in next stage 1 after bud burst. It was demonstrated that leaf phosphate is directly reused for new tissues in the next growing season.

Based on the above results, the present study gives an outline of seasonal utilization of phosphate in deciduous woody plant; *Populus alba* as follows.

In growing season, a main form of phosphorus is inorganic phosphate in various tissues. Shoot apex and young leaves are the prior sink tissues. Phosphate is re-translocated to the young sink tissues from older tissues via mainly phloem, and supports new growth. Phloem-xylem exchange also occurs, and contribute P circulation in a whole tree. In senescing season, perennial tissues work as the prior sink. P was remobilized from senescing leaves and stored in parenchyma cells in xylem and phloem in twigs. In winter, P was accumulated in electron-dense globoid-like structure in protein storage vacuoles. $IP_6$ is the main compound for winter P storage. In early spring, stored $IP_6$ was decomposed immediately, and released Pi was re-translocated again to new growing tissues.

These annual recycle of P enables deciduous trees to retain and enlarge its P pool year by year, and contribute to their long-lasting survival and huge biomass.

In the present dissertation, the following data are quotated from my master's thesis and already published paper (Kurita et al., 2014). Fig. 1, 9, 10A, 10B.

## ■ Chapter 1　Annual re-translocation and storage of phosphate in field-growing poplar trees

### Introduction

In woody plants, seasonal remobilization of nutrients has been studied for a long time since this process is important for plants to survive in nutrient-limited environments (Chapin and Kedrowski, 1983; Cherbuy et al., 2001; Keskitalo et al., 2005). Both deciduous (e.g. birch, alder, larch, poplar) and evergreen (e.g. spruce, oak) trees are known to remobilize various nutrients such as carbon (C), nitrogen (N), phosphorus (P), and sulfur (S) from senescing leaves before leaf fall. Remobilization of nutrients from senescing leaves enables plants to reuse them without absorption from the soil. Residual nutrients, which are not remobilized from leaves, can be ecologically recycled through litter. However, decomposition and re-mineralization of the litter are necessary before these nutrients become available to plants. Zeller et al. (2000) reported that about 2% of the original litter N was accumulated in the beech tree during 3 years in a beech forest. It is an advantage for perennial plants to retain nutrient within themselves by means of remobilization. The stored nutrients highly contribute to the new growth of the following year. In sessile oak [*Quercus petraea* (Matt.) Liebl.], remobilized N contributed ~90% of total N in new growing shoot during the first 2 weeks following bud burst (El Zein et al., 2011).

Among these remobilized nutrients, phosphorus is one of the precious elements, whose supply is often limited in natural environments. Phosphorus fertilizer is therefore indispensable in agriculture, but the global phosphate reserves which is usable for human activities are being depleted. There is fear that phosphorus ore that is mined

for fertilizer or engineering material may run out within a century, which is called as "phosphate crisis" (Abelson, 1999). To mitigate or avoid this potential crisis which is a serious threat for the sustainability of human society, it is important to investigate ways of reducing applied phosphate for the requirements of agricultural plants. Plants have well developed mechanisms for internal recycling of phosphate, often involving seasonal storage in permanent tissues. Phosphorus remobilization from older to younger tissues has been extensively investigated (Biddulph et al., 1958a; Mimura et al., 1996; Fujii et al., 2005; Chiou et al., 2006; Lin et al., 2009).

Seasonal recycling of phosphate in woody plants is also one of the mechanisms to adapt phosphate deficiency. Previous studies showed that phosphorus was remobilized from senescing leaves in deciduous trees during autumn (Chapin and Kedrowski, 1983; Aerts, 1996; Keskitalo et al., 2005). Nutrient remobilization is a conserved mechanism in various species, and the mean P resorption efficiency (% of the leaf P pool resorbed) was 50.4% in deciduous shrubs and trees (n=98)(Aerts, 1996). In a kind of deciduous tree, *Populus tremura*, about 80% of phosphorus was remobilized during autumn senescence (Keskitalo *et al.*, 2005). It was shown that some members of phosphate transporter family; *PHT1* in poplar (*PtPT1, PtPT5, PtPT6, PtPT9,* and *PtPT12*) were strongly up-regulated in the oldest leaves undergoing autumnal senescence, and suggested that they play a role in Pi remobilization from leaves (Loth-Pereda et al., 2011). Remobilized phosphorus is supposed to be stored in perennial tissues during winter. In Poplar woods, it is known that the ray cells are main storage parenchyma for C and N. The three main storage subcellular structures ( i.e. protein storage vacuole, lipid body, starch granule) were found in xylem ray cells in 3-year-old twig during late autumn (Sauter and van Cleve, 1994).

In deciduous taiga trees, it was reported that phosphorus was stored in buds

and current stems during winter as phospholipids, non-hydrolyzable esters, and nucleic acids, but the amount of $IP_6$ was negligible (Chapin and Kedrowski, 1983). Thus far, the molecular form of storage and the storage tissues of phosphorus in temperate deciduous trees have not been clarified.

## Materials and methods

### Plant materials

In the analyses of the field plants, leaves were sampled every month between 13:30 to 14:30 PM from April, 2010 to November, 2011, from a field white poplar (*Populus alba*: TreeA) at Uji Campus of Kyoto University (34°91'N, 135°80'E, elevation 24 m). Leaves were sampled at the height between 1 m and 2.5 m from the ground. Fresh weight of each sample was measured, and then samples were frozen in liquid nitrogen. Leaf samples were stored at -20 °C until the extraction of phosphates.

New twigs that sprouted in the current year and one-year-old twigs of white poplar were collected between 13:30 to 14:30 PM from March 2012 to February 2014. The twigs from March 2012 to February 2013 and those from April 2013 to February 2014 were collected from different trees (Tree A and Tree B), respectively. The two trees were 8-years-old in 2012, and stood side by side. Twigs at the height between 1 m and 2.5 m from the ground were collected. Twigs were separated into new twigs and one-year-old twigs which distinguished by the node of the branch.

New twigs of *Acer palmatum* Thunb., *Zelkova serrata*, *Rhaphiolepis indica var. umbellata* (Thunb.) H. Ohashi and *Viburnum odoratissimum var.* awabuki (K. Koch) Zabel ex Rumpler were collected in February 2015 at Rokkodai Campus of Kobe University. (34°72'N, 135°23'E, elevation 162 m). Because it was difficult to judge the ages of twig (newly grown or one-year old) of *Hydrangea macrophylla* (Thunb.) Ser., twigs were collected within 10 cm from shoot apex.

The fresh weight of each sample was measured immediately after the collection, and then their dry weights were measured after freeze-drying with FreeZone (FZ-1, Labconco, Kansas, USA) for 1 day. Samples were frozen in liquid nitrogen and

stored at -20℃ until measurements.

**Extraction of inorganic and organic phosphates**

Frozen fresh leaves were ground with a mortar and pestle in liquid nitrogen. Dried twigs were cut into small pieces, and then homogenized by homogenizer (SH-48, KURABO, Osaka, Japan) or Multi-Beads Shocker (MB601KU, Yasui Kikai Co., Osaka, Japan). Homogenized samples were soaked in water. The homogenate was centrifuged at 20,400 g for 10 min at 4°C (MX-301, TOMY, Tokyo, Japan). The supernatant was boiled for 7 min at 98°C (DRY THERMO UNIT TAH-1G, TAITEC, Saitama, Japan), and again centrifuged at 20,400 g for 10 min at 4°C. The supernatant was filtered through 5.0 μm Ultrafree centrifuge filter (UFC30SV00, Millipore, MA, USA) at 5,000 g for 3 min at 4°C. The extract was stored at -20°C until measurement.

**Measurements of inorganic and organic phosphates**

Inorganic phosphate was measured by the molybdenum blue method (Murphy and Riley, 1962). Total phosphorus was measured by the molybdenum blue method after degradation of organic phosphates by potassium persulfate oxidation. Organic phosphate was calculated by subtraction of inorganic phosphate (Pi) value from total phosphorus value.

-Potassium persulfate oxidation-

To adjust final concentration within measurable range of the molybdenum blue method (absorbance: 0.05~0.2), every sample extract was diluted with appropriate volume of $H_2O$. The diluted solution was added to potassium persulfate solution (5 g/100 ml $H_2O$) in a volume ratio of 1:4, and heated in an autoclave at 120°C for 90 min.

After dilution by two times with $H_2O$, resolved total phosphate was measured by the molybdenum blue method.

-Molybdenum blue method-

In the molybdenum blue method, the following stock solutions were prepared (30 g/L ammonium molybdate, 254 g/L 5 N sulfuric acid, 54 g/L ascorbic acid (prepared every time before immediate use), 1.36 g/L potassium antimonyl tartrate). Just before the measurement, stock reagents of ammonium molybdate, sulfuric acid, ascorbic acid and potassium antimonyl tartrate, were mixed in a volume ratio of 2:5:2:1. The mixed reagent was added to inorganic or resolved total phosphate solution in a volume ratio of 1:10. After 60 min, the absorbance was read on a spectrophotometer (DU 730, BECKMAN COULTER, Brea, CA, USA) at 885 nm. Potassium dihydrogen phosphate was used as a phosphate standard.

**Extraction and measurement of $IP_6$**

Homogenized dried twigs were diluted with 2.4% HCl. After 30 min on ice, the homogenate was centrifuged at 20,400 g for 10 min at 4℃. The supernatant was boiled for 10 min at 98℃, and centrifuged at 20,400 g for 10 min at 4℃. The supernatant was filtered by 5.0 μm ultrafree centrifuge filter (UFC30SV00, Millipore, MA, USA) at 5,000 g for 3 min at 4℃. The filtrate was again filtered by Amicon Ultra Centrifugal Filters (UFC501096, Millipore) at 5,000 g for 60 min at 4℃. Extract solutions were diluted with $H_2O$ to make HCl levels 0.48%.

$IP_6$ was measured with an ion chromatography (DX-500, DIONEX, CA, USA) (Mitsuhashi et al., 2005). The extract was diluted with $H_2O$, and then 25 μL of the filtrate was subjected to the ion chromatography. $IP_6$ in a sample was calculated

based on a standard curve of phytic acid dodecasodium salt hydrate (SIGMA P0109, minimum 90%).

**Phytase treatment**

Phytase (SIGMA P-1259) solution (10 mg/100 μl) was added to $IP_6$ extract from new twigs collected in February. After incubation for 5 h at 55℃, sample solutions were diluted with 0.96% HCl to make HCl levels 0.48%. Sample solutions were boiled for 15 min at 98℃, and centrifuged at 15,000 rpm for 10 min at 4℃. The supernatant was filtered by 5.0 μm Ultrafree centrifuge filter at 7,400 rpm for 3 min at 4℃. The filtrate was filtered by Amicon Ultra Centrifugal Filters (UFC501096, Millipore) at 7,400 rpm for 60 min at 4℃. This treatment perfectly degraded the authentic $IP_6$ with phytase.

**Electron microscopy and energy dispersive X-ray spectrometry analysis**

Twigs were cut into small pieces (approx. 2 x 2 x 1 $mm^3$) in 20 mM potassium dihydrogen phosphate buffer at pH 7.2. These pieces were chemically fixed in 3.5% glutaraldehyde in a phosphate buffer overnight at 4℃. After being washed with phosphate buffer, samples were fixed with 1% $OsO_4$ with phosphate buffer overnight at 4℃. Samples were again washed with phosphate buffer, dehydrated in an ethanol series and embedded in Spurr's resin. The ultra-thin sections (90 nm) were cut with a diamond knife. Sections were stained with uranyl acetate and lead citrate, and observed in the transmission electron microscope (TEM) (H-7100, Hitachi Co. Tokyo, Japan).

For the energy dispersive X-ray spectrometry (EDX) analysis, post-fixation with $OsO_4$ was omitted from the chemical fixation because Os disturbs a detection of elemental P. Semi-thin sections (200 nm) were cut with a diamond knife, and analyzed

with a JEOL JEM-2100F equipped with a JED-2300T EDX system (JEOL, Tokyo, Japan).

## Results

### Annual changes in leaf phosphate contents

To confirm remobilization of phosphates from the autumn leaves, contents of inorganic and water-soluble organic phosphates (Pi and Po, respectively) in the field poplar leaves were measured from April 2010 to November 2011 (Fig. 1A). In the poplar tree in Kyoto University, Uji campus, bud break occurred in April, and then leaf expansion began. From October to November, leaves turned yellow, and fell by December. In 2010, Pi contents in leaves were nearly constant from May to August (about 3~3.5 μmol / Leaf), whereas in 2011 they generally increased from April to August. Although the Pi contents of each month in 2010 and 2011 were different, the maximum Pi content in August 2011 was nearly equal to that in August 2010. The decrease in leaf Pi contents commenced in September, and from August to November, about 75 % of Pi in leaves was remobilized (71 % in 2010, 78 % in 2011). In 2010, leaf Po content decreased continuously from May to November, and about 57 % of Po content in May was remobilized. In 2011, Po contents fluctuated throughout the year. From August to November, about 57 % of Po content in August was remobilized. Po content in October 2011 was high, resulted from the high fresh weight of sample leaves in 2011 (Fig. 1B). Po levels based on fresh weight (mmol kg / FW) showed the similar tendency, and did not show such an increase in October 2011. About 66 % and 73 % of total phosphates in leaves were remobilized in 2010 and 2011, respectively.

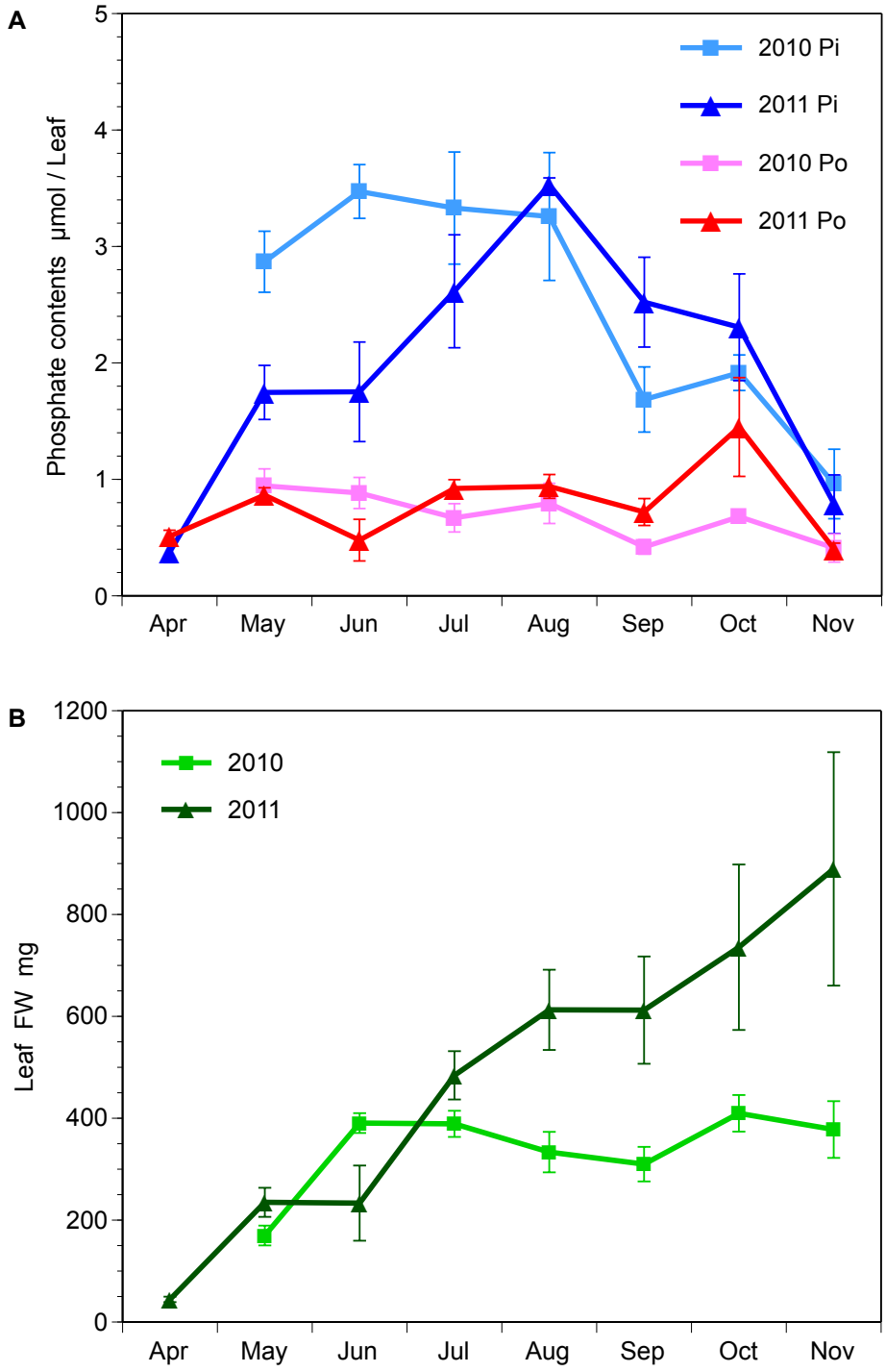


**Fig. 1** Seasonal changes in leaf phosphates and leaf fresh weight in a field poplar. (A) Seasonal changes in inorganic and water-soluble organic phosphates (Pi, Po) in poplar leaves. (B) Seasonal changes in leaf fresh weight. Pale color squares indicate measured values in 2010. Deep color triangles indicate measured values in 2011. Inorganic and organic phosphate contents are indicated by blue and red lines, respectively. (mean ± SE, n=5 in 2010, n=3 in 2011)

**Annual phosphate changes in poplar twigs**

Inorganic and water-soluble organic phosphates levels in twigs of two field-growing poplar trees (*Populus alba*) were measured over two years (Fig. 2). Pi levels were high (about 25 µmol/g DW) in summer, and sharply decreased from August to October. During winter, Pi levels were kept at low level (about 5 µmol/g DW), and again increased in spring. On the other hands, Po levels gradually increased from summer to winter, and amounted to about 20 µmol/g DW in December. In the next early spring Po levels immediately decreased to about 4 µmol/g DW. There was no big difference of phosphate levels between one-year-old twigs and new twigs and/or two individual trees. These seasonal changes of phosphate levels suggest that phosphorus is stored as Po in winter.

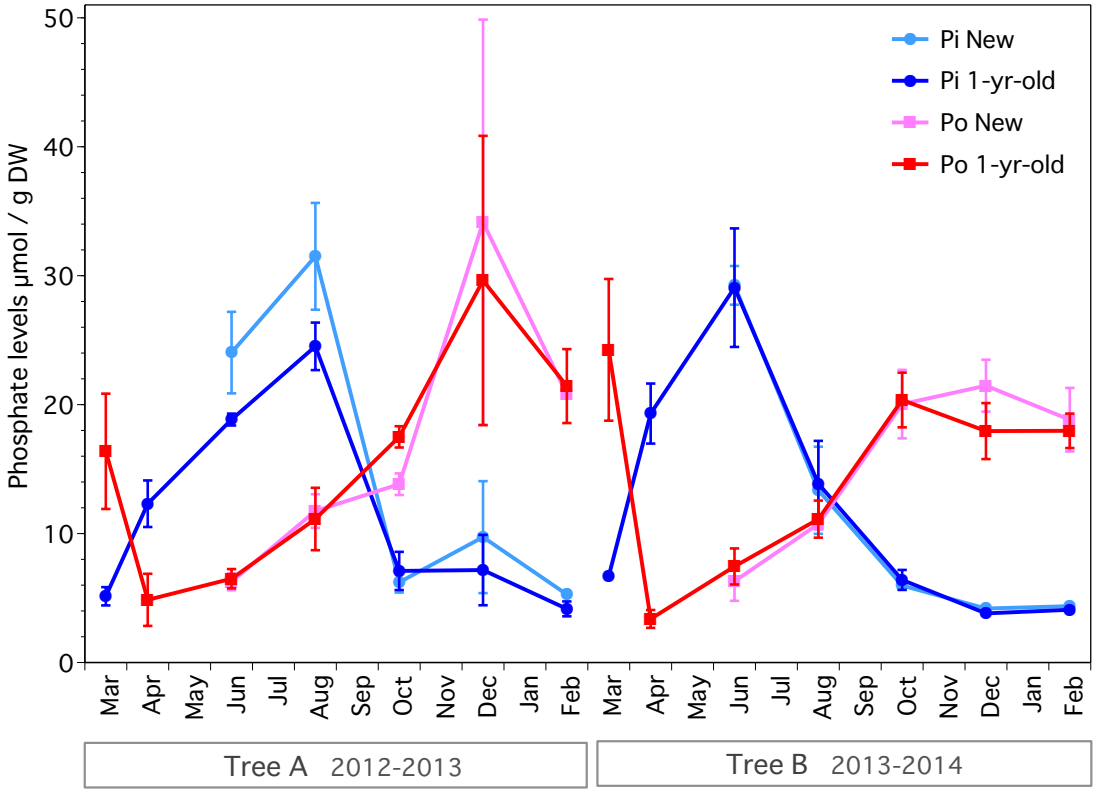


**Fig. 2** Seasonal changes in inorganic (blue circles) and water-soluble organic phosphate (red squeres) concentrations in twigs of *Populus alba*. Light and dark colors indicate measured values in new twigs and in 1-yr-old twigs respectively. (mean ± SE, n= 3, except for new twigs of February in Tree A, n=2)

**Intracellular localization of phosphorus in winter twig**

In seed cells of the angiosperm, phosphorus is stored inside the protein storage vacuole (PSV) as a electron-dense structure which is called “globoid” (Otegui et al., 2002). In the former electron microscopic observation, the presence of globoid-like structure in cells of Japanese pagoda tree (*Styphnolobium japonicum* (L.) Schott.) was noticed (personal communication from Dr. Kei’ichi Baba in Kyoto University). Thus, in order to confirm whether the globoid-like structures exist in the storage parenchyma in poplar, new twigs collected in January were observed by electron microscopy. In electron micrographs of cross section of new twig in January, ray cells and some phloem parenchyma cells were filled with protein storage vacuoles, lipid bodies and starch granules (Fig. 3A, B). Furthermore, many globoid-like structures were observed inside in the protein storage vacuoles in xylem ray cells (Fig. 3C). This structure was also observed in axial parenchyma cells in xylem, phloem ray cells, phloem parenchyma cells, and parenchyma cells in the perimedullary zone. In June, lytic vacuoles were observed instead of PSVs in ray cells. The globoid-like structure was not observed at all (Fig. 4). The elemental composition of the globoid-like structure was analyzed by Energy dispersive X-ray spectrometry analysis. Phosphorus and oxygen was detected at globoid-like structures (Fig. 5, 6). Strong signal of P was not detected at the other regions. Various cations (Ca, Mg, Na, K, Zn, Pb, and Fe) co-localized with P at globoid-like structures. Cation species and contents were different at each globoid-like structure.

Fig. S1 補足資料 ポプラ幹の横断面と組織名

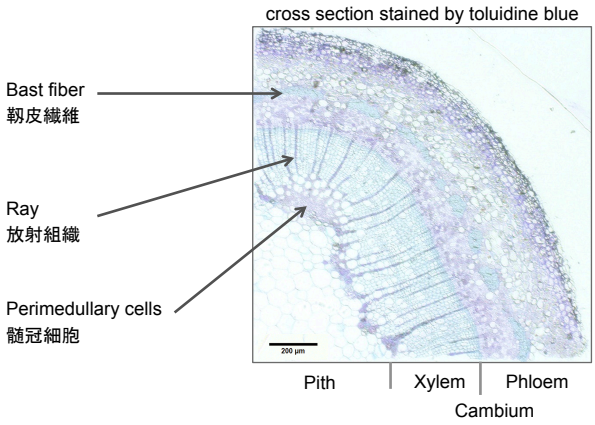


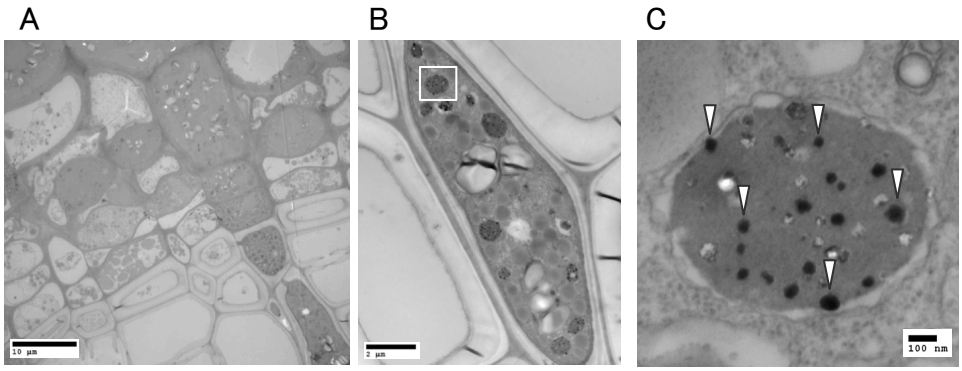


**Fig. 3** Electron micrographs of cross-section of poplar new twigs in January. **A** Ray parenchyma cells crossing the cambial region. **B** Xylem ray cell which were filled with protein storage vacuoles (PSV), lipid bodies and starch grains. **C** Higher magnification of the PSV (white box in B). There were many high electron dense globoid-like structures (arrowheads) in side PSV.

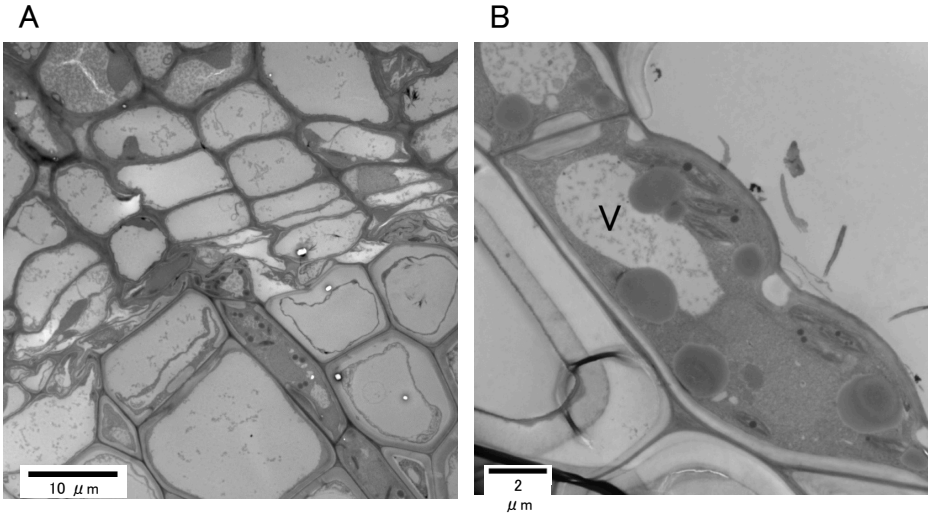


**Fig. 4** Electron micrographs of cross-section of poplar new twigs in June. **A** Ray parenchyma cells crossing the cambial region. **B** Xylem ray cell. The vacuole was lytic, and did not contain high electron dense structures. V: vacuole.

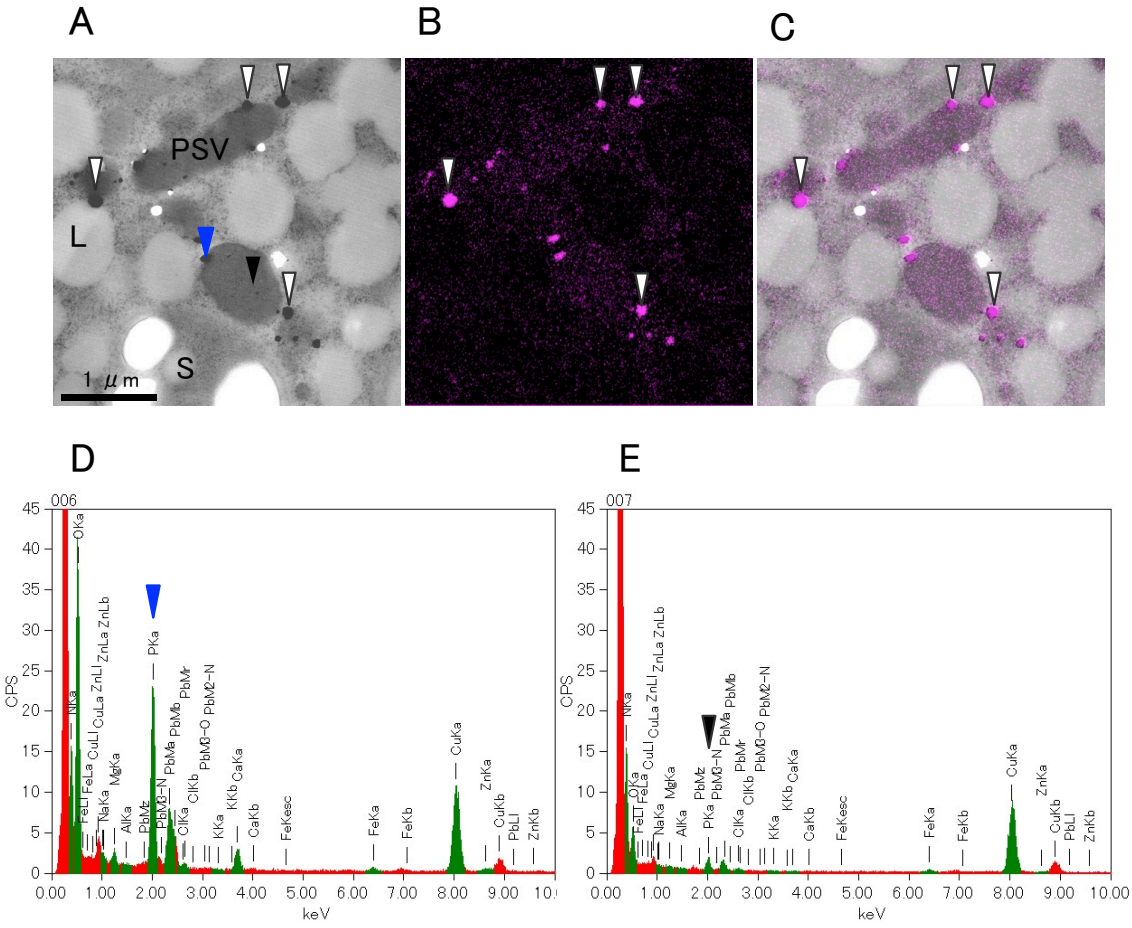


**Fig. 5** Energy dispersive X-ray spectrometry (EDXS) analysis of globoid-like structures in poplar new twigs in January. **A** High electron dense globoid-like structures (white arrowheads) inside PSVs in xylem ray cell. L: lipid body, S: starch grain. **B** Elemental mapping of phosphorus. Strong signals were observed at globoid-like structures. **C** Merged image. **D** EDXS spectrum of globoid-like structure (blue arrowhead in A). Strong peak of phosphorus (blue arrowhead) was detected. **E** EDXS spectrum in the PSV matrix (black arrowhead in A). The peak of phosphorus were slightly detected.

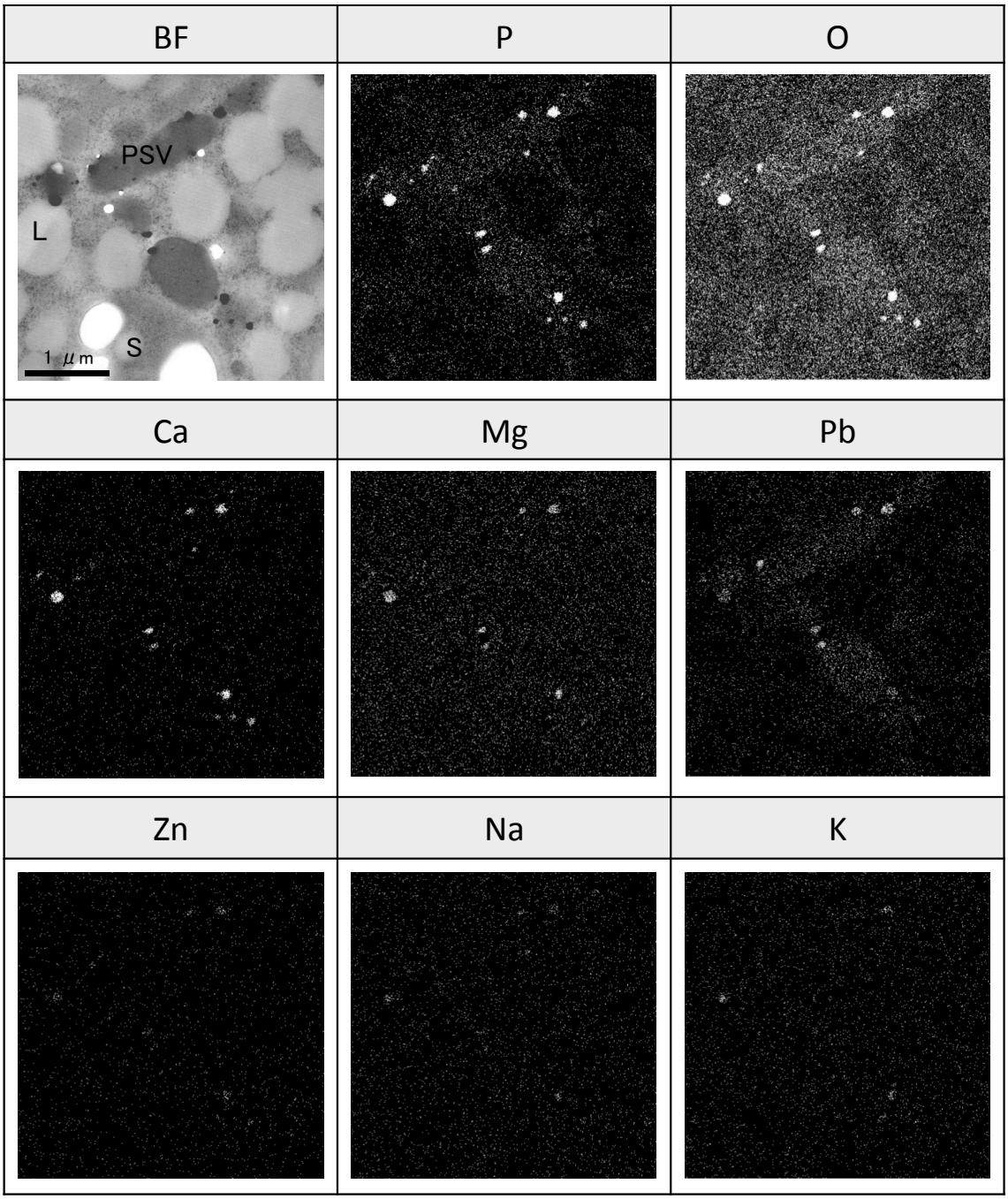


**Fig. 6** Energy dispersive X-ray spectrometry (EDXS) analysis of globoid-like structures in poplar new twigs in Junuary. PSV: protein storage vacuole, L: lipid body, S: starch grain.

**Identification of the organic phosphate compound for winter storage**

Phosphorus was found at globoid-like structures in winter twigs. It is known that at the globoids in angiosperm plant seeds, most P is stored as $IP_6$. Therefore, we assumed that $IP_6$ might be one of seasonal P storage compounds in poplar twigs. We measured the $IP_6$ in winter twigs with ion chromatography (Mitsuhashi et al., 2005). In the acid extract of twigs, a clear peak was detected close to the peak of the authentic $IP_6$ (Fig. 7A). To confirm whether these peaks are derived from $IP_6$, samples treated with phytase which can hydrolyze inositol phosphates to inositol and inorganic phosphates were measured. The sample peak, which was detected close to the $IP_6$ disappeared by phytase treatment (Fig. 7A). Thus, it is strongly suggested that the peak was derived from $IP_6$.

$IP_6$ levels in twigs showed the same seasonal pattern as that with Po levels in twigs (Fig. 2, 7B, 8). In new twigs grown from 1-year-old twig, $IP_6$ levels gradually increased from June to December, and amounted to about 7-8 μmol/g DW. During the early spring, $IP_6$ level in 1-year-old twigs sharply decreased (less than 1 μmol/g DW in April). Thereafter, $IP_6$ level increased again to almost the same value as new twigs. There were no significant differences of $IP_6$ levels between Trees A and B. In most cases, the values of contents of inorganic phosphate calculated from $IP_6$ were exceeded Po value (Fig. 8)

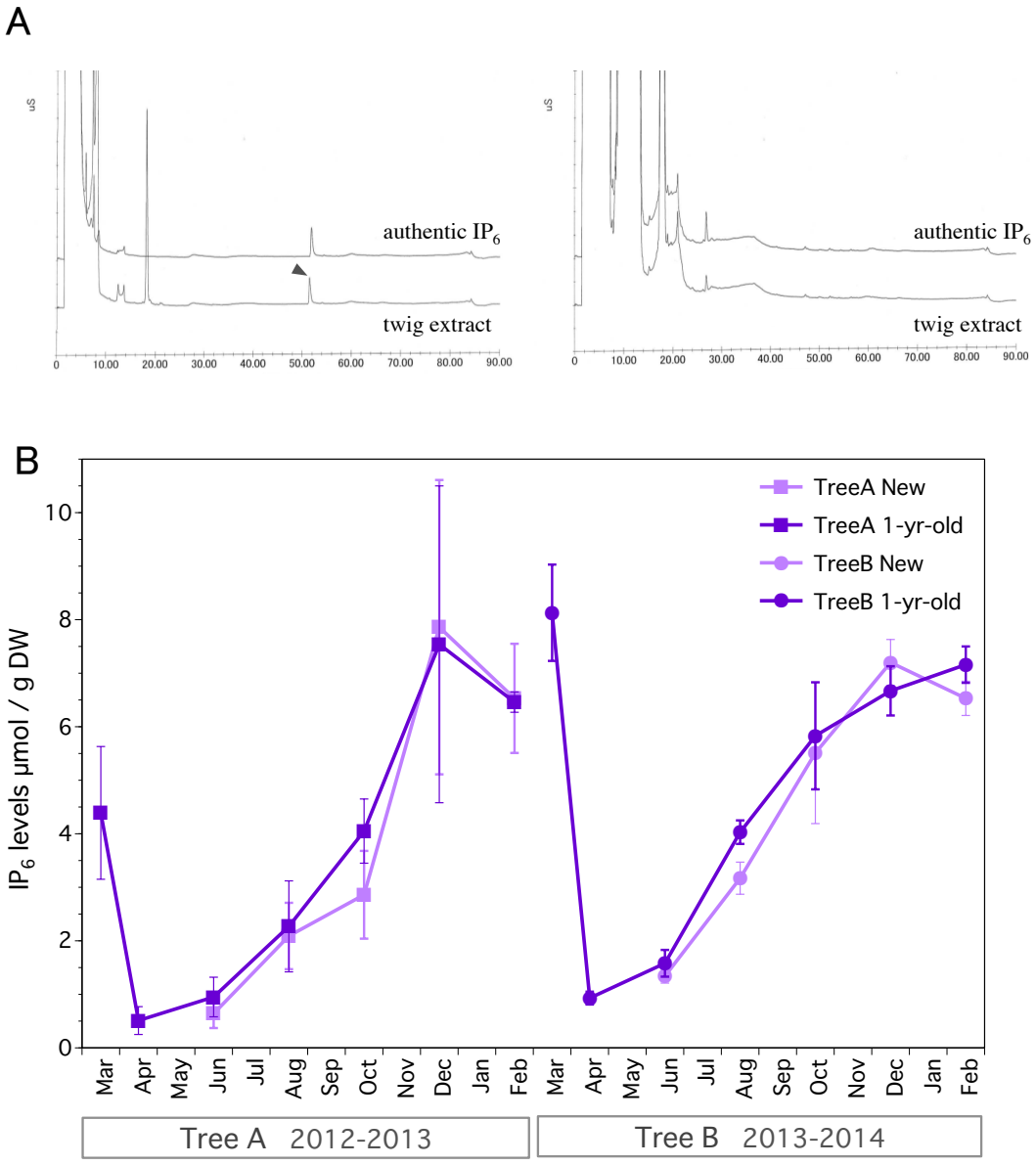


**Fig. 7** **A** Ion chromatograms of extracts of the poplar new twig in February and the authentic $IP_6$ (left). The retention time of a peak of the winter twig extract was almost the same as that of the authentic $IP_6$ (arrowhead). By phytase treatment, these peaks disappeared (right). **B** Seasonal changes in $IP_6$ concentration in twigs in *Populus alba*. Squares and circles indicate measured values in Tree A (2012-2013) and B (2013-2014), respectively. Pale colors and deep colors indicate measured values in new twigs and in 1-yr-old twigs, respectively. (mean ± SE, n= 3)

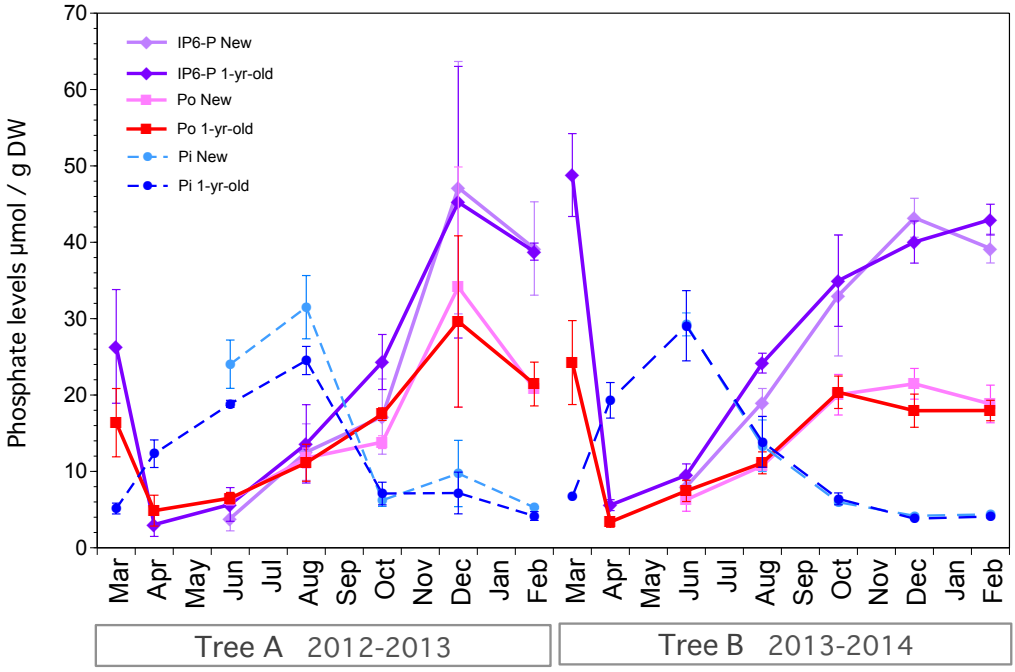


**Fig. 8** Comparison between Pi and Po concentrations and the values that converted $IP_6$ into inorganic phosphate in poplar twigs (mean ± SE, n= 3, Only as for the Pi and Po value in new twig of Tree A in February, n=2)

**Comparison of $IP_6$ contents of deciduous and evergreen trees in winter.**

To confirm weather $IP_6$ accumulation for winter storage is common in other tree species, $IP_6$ in new twigs of various tree species, which harvested in February, 2014, were measured in deciduous trees (*Zelkova serrata*, *Acer palmatum*, *Hydrangea macrophylla*) and evergreen trees (*Viburnum odoratissimum var. awabuki*, *Rhaphiolepis indica var. umbellata*) (Fig. 9). In deciduous trees, a definite amount of $IP_6$ (*Zelkova serrata*: 1.8 μmol/g DW, *Acer palmatum*: 0.9 μmol/g DW, *Hydrangea macrophylla*: 1.4 μmol/g DW) was accumulated in new twigs in February. On the other hand, in evergreen trees, accumulation of $IP_6$ was detected only slightly (*Viburnum odoratissimum var. awabuki*: 0.4μmol/g DW, *Rhaphiolepis indica var. umbellata*: 0.1 μmol/g DW).

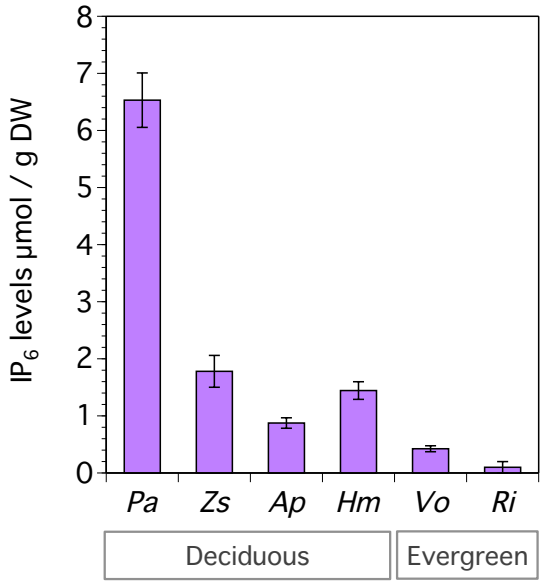


**Fig. 9** $IP_6$ concentration in new twigs in deciduous and evergreen trees in February. *Pa*: *Populus alba*, *Zs*: *Zelkova serrata*, *Ap*: *Acer palmatum*, *Hm*: *Hydrangea macrophylla*, *Vo*: *Viburnum odoratissimum var. awabuki*, *Ri*: *Rhaphiolepis indica var. umbellata*. *Pa* value is the average of measured values in 2013 and 2014 (mean ± SE, n= 3 in each year). The others are measured values in 2015 (mean ± SE, n= 3).

## Discussion

In the measurements of the field plants, remobilization of inorganic and organic phosphates from senescing leaves occurred in late summer and autumn (Fig. 1). During winter, a large amount of $IP_6$ was stored in twigs in *Populus alba*. $IP_6$ is known as a phosphorus reserver in angiosperm plant seeds (Raboy, 2003). $IP_6$ was accumulated in protein storage vacuoles as high electron dense structures called globoid with various kinds of cation (Lott et al., 2000; Otegui et al., 2002). In poplar twigs, $IP_6$ levels gradually increased from summer to winter. It is expected that these $IP_6$ originated from remobilized phosphorus from senescing leaves during autumn (Fig. 1). Accumulation of $IP_6$ has already started in August (Fig. 7B). Leaf phosphate contents in *Populus alba* were kept high until August, and then started to decrease to November (Fig. 1). Therefore poplar tree seems to store excess phosphorus in twigs prior to phosphate remobilization from leaves in autumn. During winter, phosphorus was accumulated at high electron dense structures (globoid-like structures) in the protein storage vacuoles with various kinds of cation (Ca, Mg, Zn, Na, K, etc.) in parenchyma cells in twigs as known in seeds (Fig. 5, 6). In spring, $IP_6$ levels sharply decreased and finally almost disappeared. From these behavior, it is considered that $IP_6$ is the seasonal phosphorus reservoir in the deciduous woody plant; *Populus alba*.

In vegetative period, inorganic acid (Pi) is abundant both in poplar leaves and twigs (Fig. 1, 2). In herbaceous plant, it is known that excess Pi is sequestered and stored in the vacuole to maintain cytoplasmic Pi homeostasis (Mimura, 1995). This mechanism is probably common to poplar species during vegetative period. Namely, during vegetative period, poplar trees store excess P as Pi in vacuoles in leaves and twigs, and withdraw Pi immediately depending on its growth demand. On the other

hand, during winter, $IP_6$ was abundant in twigs. Such inversion from Pi to $IP_6$ is an osmotically advantage for plant cells for storing P, because $IP_6$ contains 6 atoms of P per molecule. Also, insoluble crystal structure of globoid may be suited for long-term storage by its stability.

Winter accumulations of $IP_6$ were also detected in twigs of some other deciduous species (*Zelkova serrata, Acer palmatum, Hydrangea macrophylla*). There is a possibility that not only poplar but other deciduous species also store P as $IP_6$ in winter. On the other hand, in some evergreen species, a small amount of $IP_6$ was detected in winter twigs. It is still unclear whether $IP_6$ accumulations in other species is involved in seasonal storage of phosphorus or not. Further experiments are necessary to clarify physiological mechanisms of P recycling by measurement of seasonal fluctuation of $IP_6$ in each species.

Recently, inositol polyphosphates are reported to play important roles in cellular regulation of plant cells like $IP_3$ or $IP_4$ in animal cells (Hatch and York, 2010). $IP_6$ is a co-factor of auxin receptor protein (TIR1) (Tan et al., 2007) and $IP_5$ is also a co-factor of jasmonate receptor protein (COI1) (Sheard et al., 2010). Thus, metabolic pathway for $IP_6$ synthesis must be common in all plant cells. In fact, various genes of enzymes for $IP_6$ synthesis are expressed in cells different from seeds (Sweetman et al., 2006), and moderate amounts of $IP_6$ was detected in various tissues (Samotus and Schwimmer, 1962; Ravindran et al., 1994; Hadi Alkarawi and Zotz, 2014). This probably means that plant cells, including cells of vegetative tissues, can synthesize $IP_6$ in their own cells. Actually, there are some reports about $IP_6$ content in green leaves (Hadi Alkarawi and Zotz, 2014), further reported that foliar $IP_6$ represented, on average, 7.6% of total P. Deciduous trees must have acquired the ability to utilize $IP_6$ for seasonal storage. I have not succeeded to identify the tissues where $IP_6$ are synthesized

in the present study. The possibilities that $IP_6$ which is synthesized in leaves will be transported to perennial tissues and/or remobilized P will be synthesized to $IP_6$ in perennial tissues, are supposed.

Discovery of $IP_6$ accumulation in deciduous trees adds a new dimension to the terrestrial phosphorus cycle. In soil, most phosphorus is normally present in organic forms, of which $IP_6$ is the major component. It is generally considered that the $IP_6$ in soils originates from plants, especially seeds (Turner et al., 2002), but a significant fraction may actually be derived from the decay of trees and fallen branches.

To avert a phosphate crisis in agriculture, we need to urgently examine strategies for optimizing phosphorus use and recovery. These may include genetic construction of plants with better efficiency of phosphate use and the higher ability to internally recycle phosphorus, in parallel with more efficient mining of the phosphorus ore, industrial recovery from human activities such as from sewage treatment plants, etc. Trees represent one of the largest biomasses in the ecosystem, and consequently are a large reservoir of phosphorus. It is therefore important to understand their phosphate metabolism, both during growth and when they die. The discovery of $IP_6$ as a seasonal storage reservoir of deciduous trees is one step for such understanding.

## ■ Chapter 2 Establishment of a shortened annual cycle system in laboratory

### Introduction

Seasonal nutrients recycle in trees (remobilization, storage, reutilization) has been mostly reported using field trees (Chapin and Kedrowski, 1983; Keskitalo *et al.*, 2005; El Zein *et al.*, 2011). However, in the field condition, seasonal events, including seasonal nutrients recycle occur once a year, and may be strongly affected by the climate changes, nutrient condition and herbivory, etc. Regulation of seasonal growth-dormancy cycle in perennials and its environmental cues have been investigated intensively (Rohde and Bhalerao, 2007; Horvath, 2009; Cooke et al., 2012; Shim et al., 2014). Cessation of apical elongation growth is the initial process to dormancy. Perception of short day photoperiods induce growth cessation and transition to dormancy (Böhlenius et al., 2006; Rohde et al., 2011). In poplar, it is also suggested that temperature signals work as an additional environmental factor that modifies the sensitivity to day-length signals at growth cessation (Rohde et al., 2011). Lack of nutrients, particularly nitrogen, and drought can enhance and induce growth cessation in birch and poplar (Cooke et al., 2012). Autumn leaf senescence is also thought to be triggered by the reduction of photoperiod, and accelerated by low temperature (Keskitalo et al., 2005; Fracheboud et al., 2009). It was suggested that bud set and autumn senescence appeared to be under the control of two different critical photoperiod, however, bud set and growth cessation are prerequisite process for the initiation of autumn leaf senescence (Fracheboud et al., 2009). Further, release from dormancy requires exposure to chilling temperature. After chilling, exposure to higher temperature is considered to be necessary for dormancy release.

In order to clarify cellular and molecular mechanism of phosphate utilization and remobilization of trees as shown in Chapter 1, we have to overcome the complexities in the field condition. In the present study, a model system of seasonal phosphate re-translocation in deciduous trees under laboratory conditions (= 'shortened annual cycle') was established.

## Materials and methods

### Plant materials and culture condition.

Poplar shoots with 5 leaves were cut and rooted with 1/5 MS medium containing 0.1 mg/L indole butyric acid (IBA), and transferred into the pots containing vermiculite, which was washed by tap water ten times and by distilled water five times. Potted cuttings were placed in tree culture chambers (LH-350S, NK system, Osaka, Japan) in turn from stage 1 to 3 under the conditions in Table 1.

Plants were fertilized with 1/5 MS medium (1L / 6 potted cuttings) once a week at stage 1. Afterwards they were cultured with distilled water only.

**Table 1.** Culture conditions in shortened annual cycle

| | Temperature | Day / Night | Incubation period | Mimicked season |
|---|---|---|---|---|
| Stage 1 | 25°C | 14 h / 10 h | 1 month | spring / summer |
| Stage 2 | 15°C | 8 h / 16 h | 1 month | autumn |
| Stage 3 | 5°C | 8 h / 16 h | 2 to 3 months | winter |

In the shortened annual cycle analysis in a laboratory, leaves were sampled from potted *Populus alba* clones in the last day of each culture stage (See Culture condition). Leaves were numbered from apical to basal. Younger leaves whose length is smaller than 3 cm were not counted.

Fresh weight of each sample was measured, and then samples were frozen in liquid nitrogen. Samples were stored at -20 °C until extraction of phosphates.

**Extraction of inorganic and organic phosphates**

**Measurement of inorganic and organic phosphates**

**Extraction and measurement of $IP_6$**

Above three methods are the same as shown in Chapter 1.

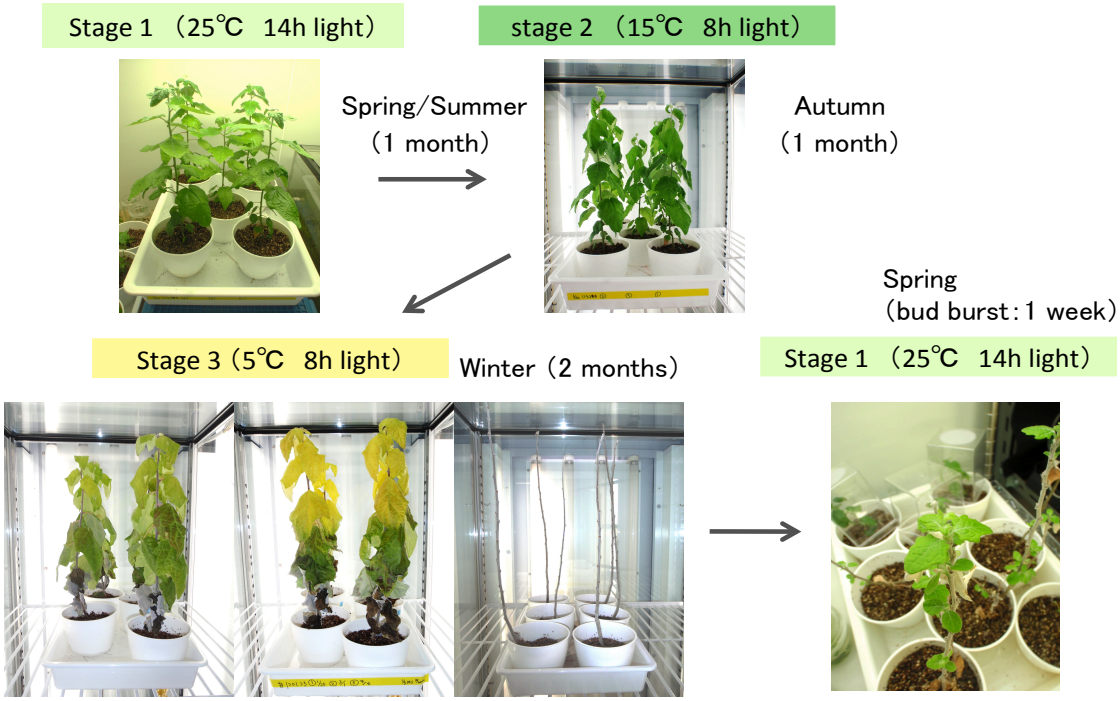


**Fig. 10** States of poplar trees In the shortened annual cycle system. Leaf coloration, leaf fall and bud break were induced by modification of temperature and day length within 5 to 6 month.

## Results

### The poplar growth in shortened annual cycle

Popular shoots were planted in pots and grown at 25 °C with 14 h light (c.a. 200 μmol/$m^2$s) for 1 month to represent spring and summer conditions (**stage 1**). In this system, phosphate contents in leaves depend on the amount of fertilized P. To approximate phosphate contents of laboratory poplar to those in the natural leaves during growing season (3-4 μmol/Leaf), plants were fertilized with 1/5 MS medium once a week during stage 1 (1L/6 potted cuttings). Then, to acclimatize to low temperature and short lighting conditions, trees were transferred to 15 °C with 8 h light (c.a. 30-40 μmol/$m^2$s) and cultured for 1 month to represent autumn conditions (**stage 2**). Finally, trees were cultured at 5 °C with 8 h light (c.a. 30-40 μmol/$m^2$s) for 2 to 3 months to represent winter conditions (**stage 3**). Table 1 summarizes these conditions.

During stages 1 and 2, trees were growing, and increased the number of countable leaves. Approximately 12 leaves developed during stage 1 and around four leaves developed during stage 2. It is that the first leaf at the end of stage1 corresponds to the third to fifth leaf at the end of stage 2. During stage 3, the number of leaves increased by no more than two. At that time, although the trees seemed to stop shoot apical growth, the leaf number increased only by expansion of uncounted small leaves in the preceding stage. Thus, the total number of leaves in the tree sapling before leaf fall became about 23, compared to around 5 at the beginning of culture (see M & M). In stage 3, leaf coloration and leaf fall occurred in the upper leaves, while the lower leaves did not show yellow color and withered. When defoliated trees were again moved to condition of stage 1, new leaves emerged within one or two weeks.

**Stage-dependent changes of leaf phosphate contents in the shortened annual cycle**

To measure phosphate distribution in poplar trees in this system, Pi and Po contents in leaves were measured along the shoot axis (Fig. 11A). In stage 1, except for the 1st leaf, Pi and Po contents per leaf were higher in young upper leaves than in lower leaves. The 1st leaf was not mature (small and not fully expanded), and its fresh weight (the 1st: approximately 137 mg) was smaller than lower-positioned leaves (the 5th: 527 mg). However, phosphate levels of the 1st leaf (Pi: 8.3 mmol/kg FW, Po: 7.4 mmol/kg FW) was roughly the same value as the 3rd leaf (Pi: 8.9 mmol/kg FW, Po: 5.7 mmol/kg FW), and higher than that of the 5th leaf (Pi: 6.0 mmol/kg FW, Po: 2.6 mmol/kg FW) and those of downward ones. In stage 2, Pi and Po contents were also higher in young upper leaves than in lower leaves. However, Pi contents in leaves were lower than in stage 1. In stage 3, Pi and Po contents decreased greatly in the 5th to the 7th leaves. This shows that the efficiency of remobilization of phosphate varies according to the leaf position from the apex or leaf age.

The 1st leaf at the end of stage 1 became the 3rd to 5th leaf at the end of stage 2. Phosphate contents in this leaf increased during stage 2. Phosphate contents in lower-positioned leaves (6th and 7th at stage 2 that correspond to about 3rd leaf at stage 1) decreased during stage 2 (Fig. 11A). It was presumed that changes in phosphate contents in leaves were caused by re-translocation of P (phosphorus) from elder lower leaves to younger upper leaves.

Pi and Po contents of the 6th leaf were measured in each stage under the assumption the leaves of the same position has the same capacity as the source tissue for the sink tissues (Fig.11B). It was considered that the effect of phosphate

re-translocation from old leaves to young leaves would be suppressed by using the leaves of the same position. Compared to the autumn remobilization in the field (Fig. 1A), phosphate contents in the sixth leaf of the laboratory grown plants showed a similar decrease from stages 1 to 3 (Pi: 88 %, Po: 58 %). At stage 1 of the second cycle, bud break occurred at the terminal bud and most axillary buds at the same time and Pi and Po contents in leaves increased again (Fig. 11B). At the second stage 1, it was difficult to determine the leaf position because leaves sprouted from the axial bud and lateral buds. Therefore, leaves were collected randomly from trees at the second stage 1.

$IP_6$ levels in the stem were measured in each stage (Fig. 11C). In stage 1, $IP_6$ level in the stem was quite low (less than 1 μmol / g DW). In stage 2, $IP_6$ level increased a little. In stage 3, $IP_6$ level greatly increased, and reached the same value as field-growing poplar twigs in winter (Fig. 7B, 11C). At stage 1 of the second cycle, $IP_6$ level sharply decreased and became almost zero.

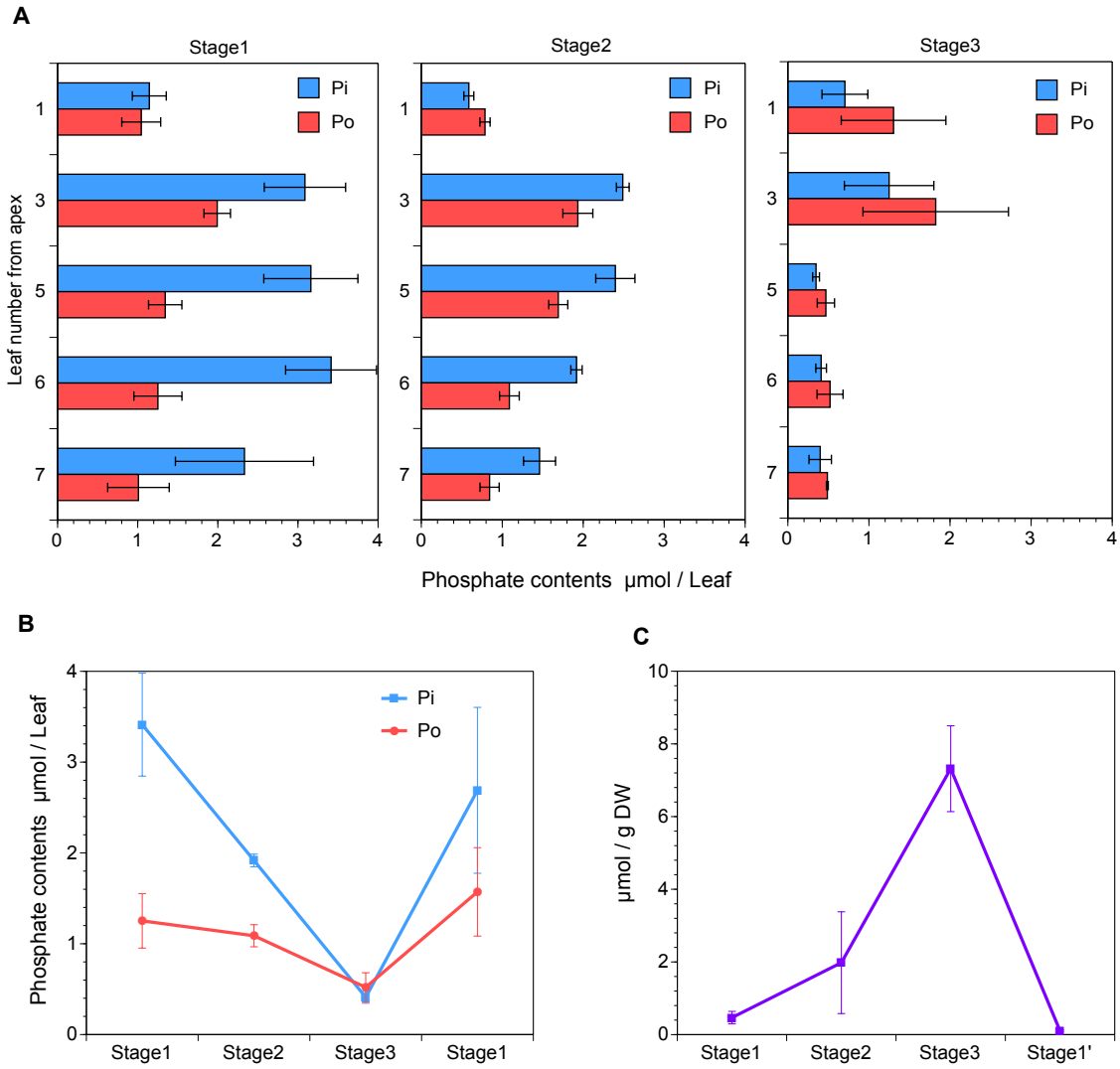


**Fig. 11** Phosphate contents and concentrations in poplar in the shortened annual cycle system. **A** Leaf phosphate contents along shoot axis. Leaves were numbered from apical to basal. Immature leaves smaller than 3 cm were not counted. **B** Changes in phosphate contents in 6$^{th}$ leaves during stage 1 to 3, and second stage 1. Inorganic and organic phosphate contents are indicated by blue and red bars or lines, respectively. **C** Changes in $IP_6$ concentration in stem during stage 1 to 3, and second stage 1. (mean ± SE, n= 3)

## Discussion

In nature, in deciduous plants, seasonal events like leaf fall and bud break occur only once a year and these events are strongly influenced by various environmental factors as temperature, rainfall, day length, etc. This complicates analysis of molecular processes that contribute to re-translocation within the plant and remobilization during senescence. In an attempt to control the phenological phenomena, we have established and tested a controlled environmental system that mimics the developmental events that occur under field conditions. The main differences of this new system from the field condition are that the phenology is more predictable, and the annual cycle can be achieved within approximately 5 months. This system enabled us to analyze phosphate re-translocation in a tree in a shorter period without influence of mutable climatic factors.

In this shortened annual cycle system, by controlling temperature and day length, we succeeded in reproducing changes in leaf coloration, phosphate remobilization from leaves and $IP_6$ accumulation in the stem during dormant season under field conditions (Fig. 1, 11). In the field, phosphate remobilization started in September before leaf coloration. The precise trigger for this phosphate remobilization from senescent leaves is still unclear. In previous studies, it was revealed that *Populus* responded to a critically shortened day length with the cessation of elongation growth and the formation of terminal buds (Rohde and Bhalerao, 2007; Shim et al., 2014). In the European aspen (*Populus tremula*), autumn senescence starts every year at around the same date, suggesting that the main trigger is the shortening of day length in the photoperiod (Keskitalo *et al*. 2005). In nitrogen recycling, the expression of genes of bark storage protein during autumn is also regulated by the photoperiod, through the

action of phytochrome (Zhu and Coleman, 2001). It is probable that phosphate remobilization from senescing leaves and subsequent winter storage of phosphate are also regulated by the photoperiod. However, in our measurement of field popular, it should be noted that a little amount of accummulation of $IP_6$ in twigs was already observed in June. It is still unclear whether the ability of $IP_6$ synthesis is under seasonal regulation as in bark storage protein. Further studies are required to ensure how the shortened senescence period and artificial climate control in the present study affect the proper mechanisms of phosphate re-translocation.

In this shortened annual cycle system, trees that experienced the three developmental stages bring back to stage 1 within two or three weeks, bud break occurred, and the phosphate contents in new leaves were much higher than in leaves at stage 3. At the same time, $IP_6$ accumulation in the stem during dormant season decreased mostly. It was considered that phosphate contents in these new leaves were mainly supplied from stem and/or buds because those trees were fertilized only at the stage 1 of the first cycle. However, it is also possible that some residual fertilizer remained in the soil of a pot.

From the obtained results, it was difficult to distinguish between phosphate remobilization from senescing leaves in autumn and phosphate re-translocation from old mature leaves to young upper leaves as the development of the tree. Phosphate remobilization from leaves must be influenced by the changes in physiological conditions of other sink tissues (shoot apex, root, bud, or stem). We now have a suitable system for investigation of phosphate fluxes between different tissues and the molecular processes that underlie changes in phosphate movements within the plant during its annual cycle. This system may be applicable to other seasonal events in deciduous trees, such as re-translocation of other nutrients, bud break, cambium reactivation, and

abscission layer formation. The present system will be a valuable tool for interactive approaches using both analyses of field and laboratory plants.

## ■ Chapter 3 Analysis of seasonal re-translocation of phosphate by autoradiography

### Introduction

In herbaceous plant, it was shown that P was re-translocated from old leaves to young leaves by using autoradiography (Biddulph et al., 1958a; Mimura et al., 1996). These re-translocation of phosphate between leaves is thought to occur via the phloem. Plant vascular bundle composed of xylem and phloem, and they are functioning as a path for long-distance transport. Xylem transport is upward flow from root to shoot, and driven by the transpiration stream and the root pressure. Phloem transport is generally explained by the Münch's theory as the phloem mass flow driven by an osmotically generated pressure gradient (De Schepper et al., 2013). Windt et al. (2006) measured velocities of the xylem and phloem flow in poplar, castor bean, tomato and tobacco by using NMR imaging (Windt et al., 2006). The xylem flow velocity was 1.60 ± 0.09 mm / s, and the phloem flow velocity was 0.34 ± 0.03 mm / s in poplar in the daytime. Interestingly, the phloem flow velocities measured in poplar, castor bean, tomato and tobacco were all within the same range (0.25-0.44 mm / s), irrespective of plant size and species. Schepper et al. (2013) summarized that phloem speed in angiosperm is roughly within the same range, around 1 cm / min (De Schepper et al., 2013). Both downward and upward P re-translocation via phloem from a leaf and lateral movement from the phloem to xylem were reported by using microradiographic methods in herbaceous plant, red kidney bean (Biddulph, 1956; Biddulph et al., 1958b).

In perennial woody plants, it was relatively well investigated about P remobilization from senescing leaves during autumn (Chapin and Kedrowski, 1983;

Aerts, 1996; Keskitalo et al., 2005). However, other seasonal P recycling events, for example, P re-distribution to new shoot in spring, P re-translocation during vegetative period, P re-translocation route and mechanisms, and contribution of phloem and xylem were currently unknown (Rennenberg and Herschbach, 2013).

On the other hand, internal cycling of C, N and S were well investigated (Dickson, 1989; Herschbach et al., 2012). These elements are remobilized from senescing leaves, and recycled seasonally. Dickson (1989) summarized that C transport from source leaves to sink tissues is controlled by both the vascular connections and relative sink demand. Also, C transport direction from a leaf depends on leaf position, actuality in cottonwood, mature leaves in middle part of tree exported $^{14}C$-labeled compounds bidirectionally, whereas young leaves and old leaves exported $^{14}C$-labeled compounds mainly to the apical and the basal tissues, respectively (Dickson, 1989). In beech tree, seasonal S recycling was observed. $^{35}S$ fed to a mature leaf was detected in bark and wood of trunk, branches and root during winter. In spring, $^{35}S$ decreased in the trunk and increased in buds and young beech leaves (Herschbach and Rennenberg, 1996).

In this study, in chapter 1, autumn remobilization of phosphate was observed in field growing poplar. In chapter 2, at stage 1, phosphate re-translocation from old leaves to new leaves was suggested in shortened annual cycle. On the other hand, from stage 2 to 3, phosphate was remobilized from leaves to stem, and probably converted to $IP_6$ for winter storage. These results suggest that the phosphate re-translocation route changes seasonally. Namely, it is assumed that phosphate is re-translocated from old leaves to new leaves in growing season, while phosphate is remobilized from leaves to stem (twigs) in senescent season. To clarify this assumption, phosphate re-translocation route and its accumulation were visualized by autoradiography in shortened annual

cycle, which was developed for laboratory analysis of field phenology.

The autoradiography itself is a traditional method to observe ion distribution. To detect radio radiation, x-ray film has been used for a long time. Since 1990s, an imaging plate (IP) developed by FUJI Film Co. Ltd became utilized because IP could drastically shorten the exposure time, sometimes from a few months to a few hours. However, as long as we use both x-ray film and imaging plate, it is difficult to observe the real time course of phosphate re-translocation. As the solution to this problem, real-time radioisotope imaging system (RRIS) has been developed (Kanno et al., 2012; Hirose et al., 2013; Sugita et al., 2013). This system enables us to visualize translocation of radio-labeled compounds between organs at a whole-plant scale.

On the other hand, to observe distribution of radio-labeled compounds at cellular level, microautoradiography (MAR) technique was used, even in poplar tree (Dickson et al., 1985; Bücking and Heyser, 2001). However, these experiment need procedure of freeze-drying and the substitution with resin. Recently, a new convenient MAR protocol for fresh-frozen plant sections was developed (Hirose et al., 2014). This protocol enables us to observe the distribution of radio-labeled soluble compounds without diffusion at the cellular level.

In the present study, the imaging plate, RRIS and MAR were used to analyze seasonal re-translocation of phosphate in poplar trees.

## Materials and methods

### Plant Materials

Poplar plants were cultured in a shortened annual cycle system. In stage 1 and 2, plants at 3$^{rd}$ to 4$^{th}$ week, in stage 3, plants at 3$^{rd}$ to 5$^{th}$ week were used for the experiments.

### Whole plant autoradiography using imaging plate

To add radiophosphorus, a "flap" was cut along a vein of 6$^{th}$ leaf in the manner shown in Fig. 12, and 5 µl Phosphorus-32 ($KH_2{}^{32}PO_4$) solution with 0.2 M $KH_2PO_4$ (final concentration of 200 Bq / µL ) was added as described (Salisbury and Ross, 1992). Then, plants were cultured in each stage condition for 1 day. After 1day culture, 6$^{th}$ leaf was cut off because its strong signals disturb the measurement. The vermiculite was washed away from poplar roots with tap water. Plants were then mounted on the paper, and wrapped with double layers of polyvinyl film. The sample was set on the imaging plate in the cassette case and exposed in a dark room for 3 days. Then, the imaging plate was measured using Typhoon FLA 9500 (GE Healthcare UK Ltd., Buckinghamshir, England).

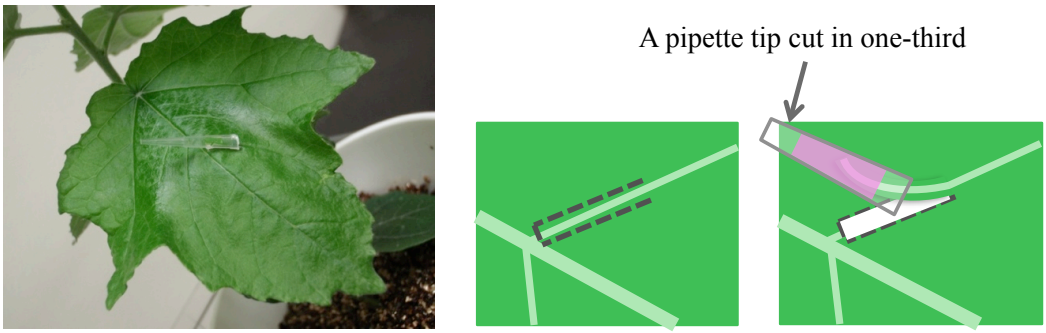


**Fig. 12** How to apply $^{32}P$ to the 6$^{th}$ leaf. A "flap" was cut along a vein from basal direction. The flap was covered with a pipette tip containing $^{32}P$ solution.

**Whole plant autoradiography using imaging plate with phloem girdling**

The bark of upper or lower internode of the 6$^{th}$ leaf was peeled off approximately 2 mm width by razor to interrupt phloem transport (Fig. 16C). Then, immediately, 5 μl Phosphorus-32 ($KH_2{}^{32}PO_4$) solution with 0.2 M $KH_2PO_4$ (final concentration of 1 kBq / μL ) was added to the 6$^{th}$ leaf as described above. Plants were cultured in stage 1 for 3 h or 1 day. After culture, 6$^{th}$ leaf was cut off. Upper and lower internodes of 6$^{th}$ leaf were cut to prevent re-translocation of $^{32}P$ during contact. The vermiculite was washed away from poplar roots with tap water. Plants were then mounted on the paper, and wrapped with double layers of polyvinyl film. The sample was set on the imaging plate in the cassette case and exposed in a dark room for 1 day. Then, the imaging plate was measured using Typhoon FLA 9500.

**Whole plant autoradiography using imaging plate over dormancy period**

Seven μl Phosphorus-32 solution with 0.2M $KH_2PO_4$ (final concentration of 700k Bq / μL ) was added to 6$^{th}$ leaf of a plant at 4$^{th}$ week in stage 3 as described above. After leaf fall, an imaging plate was attached to the plant and exposed over night. The imaging plate was wrapped with double layers of polyvinyl film to prevent contamination. Then plant was moved to stage 1 and cultured. After bud burst, the vermiculite was washed away from poplar roots with tap water. The plant was then mounted on the paper, and wrapped with double layers of polyvinyl film. The sample was set on the imaging plate in the cassette case and exposed in a dark room for 1 day. Then, the imaging plate was measured using Typhoon FLA 9500.

**Imaging using the real-time radioisotope imaging system**

To add radiophosphorus, a "flap" was cut along a vein of 6$^{th}$ leaf, and 5 μl Phosphorus-32 ($H_3{}^{32}PO_4$) solution with 0.2M $KH_2PO_4$ (final concentration of 200 kBq / μL) was added. After 1 or 3 min, a flap was cut off because its strong signals disturb the measurement. Then, plant was mounted on a fiber optic plate coated with CsI (Tl) as a scintillator and was formed through vapor deposition onto the plate of 50 μm thickness (FOSs, 100 mm × 100 mm × 5 mm, Hamamatsu Photonics Co., Hamamatsu, Japan). The mechanism of $^{32}P$ visualization is as follows: beta rays emitted from $^{32}P$ in a sample that is mounted on the FOSs interacts with the CsI (Tl) scintillator, and then is changed to visual light. Light was captured by the cooled CCD camera with an image capture system (Aquacosmos/VIM system; resolution: 640 pixel × 480 pixel, Hamamatsu Photonics Co.) (Sugita et al., 2013). The measurement was performed for three hours in the dark room at 20 °C.

**Microautoradiography (MAR) of distribution of radio-labeled compounds at cellular level,**

**-Radioisotope addition for fresh-frozen sections of cultured popular tree.**

To add radiophosphorus, a "flap" was cut in the manner shown in Fig. 11, and 5 μl Phosphorus-33 ($H_3{}^{33}PO_4$) solution with 0.2M $KH_2PO_4$ (final concentration of 37 or 74 kBq / μL) was added. Then, plants were cultured in each stage condition for 1 day.

**-Preparation of fresh-frozen sections**

Preparation of fresh-frozen sections was performed after Hirose et al. (2014) as follows.

Sectioning was performed using the Cryo-Film transfer kit (SECTION-LAB Co. Ltd., Hiroshima, Japan) as described previously (Kawamoto, 2003; Hirose et al.,

2014). Stem samples that was cut out from poplar in each stage were frozen with liquid nitrogen. The frozen stem samples were embedded in a dedicated embedding medium (SCEM; SECTION-LAB Co. Ltd.) and The frozen stem samples were serially sliced into 20 μm thick sections using a Cryostat (CM1850; Leica Microsystems, Wetzlar, Germany) set at -20°C. After the targeted tissue appeared, the surface was tightly covered with adhesive film (Cryo-Film type 2C(9); SECTION-LAB Co. Ltd.) and then carefully sliced to produce fresh-frozen sections.

**-Preparation of the glass slide coated with photosensitive nuclear emulsion**

Preparation of the glass slide coated with photosensitive nuclear emulsion was performed after Hirose et al. (2014) as follows.

The photosensitive liquid nuclear emulsion (Ilford Nuclear Emulsion Type K5; Harman Technology Ltd., Cheshire, UK) was melted at 45°C, after which 0.08% (w/w) sodium di (2-ethylhexyl) sulfosuccinate was added. To form an emulsion membrane, the hydrophilic amino-coated glass slide (MAS- GP type A; Matsunami Glass Ind., Ltd., Osaka, Japan) dipped into the melted emulsion and subsequently withdrawn. After the emulsion on the glass slide dried, the slides were subsequently used for MAR or otherwise stored in a light-tight box with silica gel for a maximum of 1 month. It should be noted that all of these processes were conducted under a safe light, and the room temperature was maintained at 20°C.

**-Exposure to the photosensitive nuclear emulsion**

Exposure to the photosensitive nuclear emulsion was performed after Hirose et al. (2014) as follows.

The emulsion-coated glass slides were put on a 1.5 mm thick aluminum plate,

tightly sealed with 1.2 μm thick polyphenylene sulfide film (One-touch film; ING Co. Ltd., Saitama, Japan), and then placed in the freezer before the MAR experiment for pre-cooling. Additionally, some clamps and another aluminum plate on which a 3 mm thick urethane foam sheet was pasted were also pre-cooled in the freezer. After pre-cooling, the fresh-frozen sections were put on the emulsion with the polyphenylene sulfide film slipped in between them. Then, the pre-cooled aluminum plate with the urethane foam sheet was lowered onto the adhesive film-carrying sections on the other side to sandwich the sections and glass slides between the two aluminum plates. The sandwich was then further wrapped in aluminum foil and pressed using clamps. These setting operations were performed in the cryostat set at -20 °C in the dark room. After the setting was complete, the sample was put in the freezer at -80 °C for exposure about 1 month or further period. The results hardly changed when the sample was exposed over 1 month.

**-Development of the microautoradiographs**

Development of the microautoradiographs was performed after Hirose et al. (2014) as follows.

After the exposure, the sample was transferred to the cryostat set at -20 °C and fixing tools were immediately removed. Then, the sections were removed from the adhesive film. The glass slides coated with the photosensitive nuclear emulsion were soaked in quarter-strength D-19 developer (Eastman Kodak Co., NY, USA) for 6 min at room temperature to develop the silver particles. Then, the slides were soaked in distilled water for 1 min to stop the development, followed by exposure to 0.83 M sodium thiosulfate for 4 min for fixation. At this stage, dipping was carefully handled because the photosensitive nuclear emulsion could become soft and relatively

vulnerable to flaking. Finally, the glass slides were soaked in distilled water for 10 min twice. The temperature of the darkroom was maintained at 20 °C to ensure development.

The sections were removed from the cryostat and floated on distilled water for 1 min three times at room temperature to wash out the embedding material. Afterward, the sections on the film were stained with 0.25 % toluidine blue for 30 sec followed by water for 1 min at room temperature. The sections were then mounted on a new glass slide using a glycerol-based mounting medium (SCMM; SECTION-LAB Co. Ltd.).

**-Microscope observation and image processing**

Microscope observation and image processing was performed after Hirose et al. (2014) as follows.

The structure of the tissues in the section and the silver particles produced in the photosensitive nuclear emulsion were observed and photographed using a microscope (BX-60; Olympus, Tokyo, Japan) equipped with an objective lens which magnified the specimen four times.

Then, the tissue images and radiographs were constructed using e-Tiling (Mitani Co., Tokyo, Japan) or ImageJ (http://rsb.info.nih.gov/ij) and its plugin, Grid/Collection stitching software (Preibisch et al., 2009). Linear contrast enhancement and registration was performed on the tissue images and radiographs using ImageJ and its plugin, Kbi Registration software (http://hasezawa.ib.k.u-tokyo.ac.jp/zp/Kbi/ImageJKbiPlugins) and GIMP software (http://www.gimp.org).

**-Autoradiography using IP for fresh-frozen sections**

Autoradiography using IP for fresh-frozen sections was performed after

Hirose et al. (2014) as follows.

Fresh-frozen sections from leaf axil of sixth leaf were prepared for autoradiography experiments using IP (BAS IP TR; GE Healthcare UK Ltd.). A previously reported protocol was followed (Kobayashi et al., 2013). The thickness of the section was 20 μm. The exposure time was about 76 h for sample in stage 1 at -80 °C. For sample in stage 3, exposure time was about 22 h because signal was strong.

After linear contrast enhancement and registration, radiographs were constructed to 3D images using ImageJ plugin Volume Viewer (http://rsb.info.nih.gov/ij/plugins/volume-viewer.html) and 3D Viewer (http://imagej.nih.gov/ij/plugins/3d-viewer/).

## Results

### Stage-dependent route of phosphate re-translocation at organ level

To visualize phosphate re-translocation from a leaf, whole plant autoradiography was performed (Fig. 13). $^{32}P$ solution was added to the 6$^{th}$ leaf. The 6$^{th}$ leaf is fully expanded and matured in this system. After 1 day culture, $^{32}P$ was detected mainly at younger leaves and apex in stage 1. $^{32}P$ was also detected at lower stem than the 6$^{th}$ leaf and at roots slightly.

In stage 2, at 4$^{th}$ week plants, two different images were obtained. One is the same as the image in stage 1. $^{32}P$ was mainly distributed at the upper parts of the plant (younger leaves and apex). Another was different from the image in stage 1. $^{32}P$ was mainly distributed at the lower parts (lower stem and roots).

In stage 3, $^{32}P$ was mainly distributed at lower stem than the 6$^{th}$ leaf and roots.

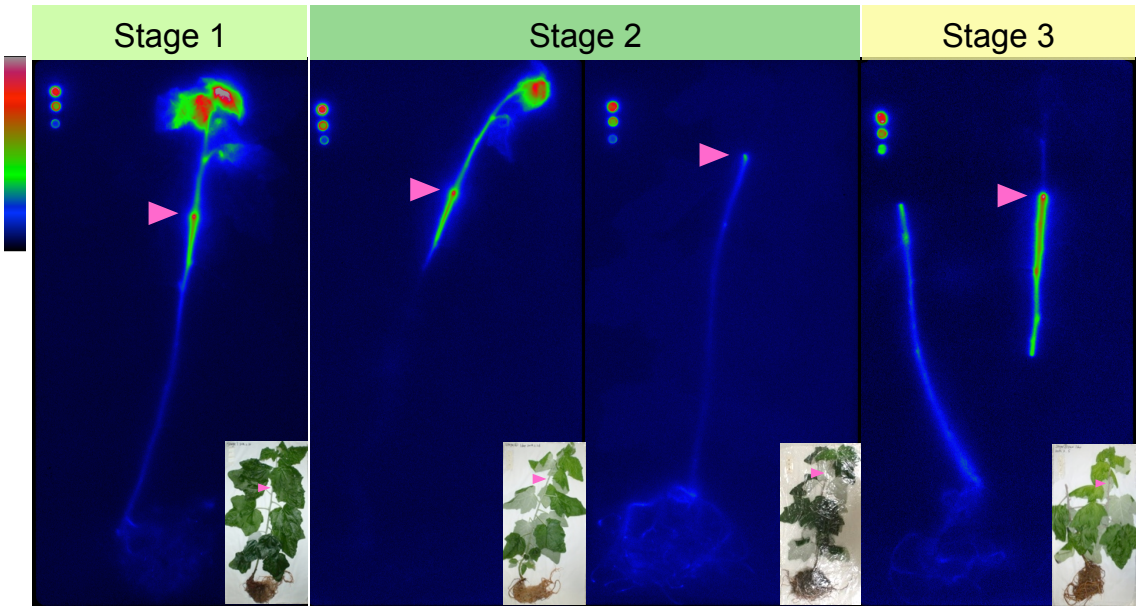


**Fig. 13** Whole plant autoradiographs in shortened annual cycle. Pink color triangles indicate the position of 6$^{th}$ leaf. The 6$^{th}$ leaf was cut off because its strong signals disturb measurement. In stage 2, two different images were obtained from plant in 4$^{th}$ week. In stage 3, stem was cut because the plant size was large for imaging plate.

**Real-time imaging of phosphate re-translocation at organ level**

To observe initial stage of phosphate re-translocation, real-time $^{32}P$ imaging was performed (Fig. 14, 15). In stage 1, weak signals were detected at the petiole of 6$^{th}$ leaf and lower stem within 15 min (Fig. 14). Then, in 30 min, signals became stronger at lower stem. At this time, signals were hardly detected at the upper part of 6$^{th}$ leaf. After 1 h and later, signals began to be detected in the upper stem, too, and became stronger over time. At least one and a half hours later, $^{32}P$-phosphate reached to the apex from 6$^{th}$ leaf.

In stage 3, signals were detected at the petiole of 6$^{th}$ leaf and lower stem in 15 min, and became stronger over time (Fig. 15). Even after 2.5 h, signals were hardly detected at the upper parts.

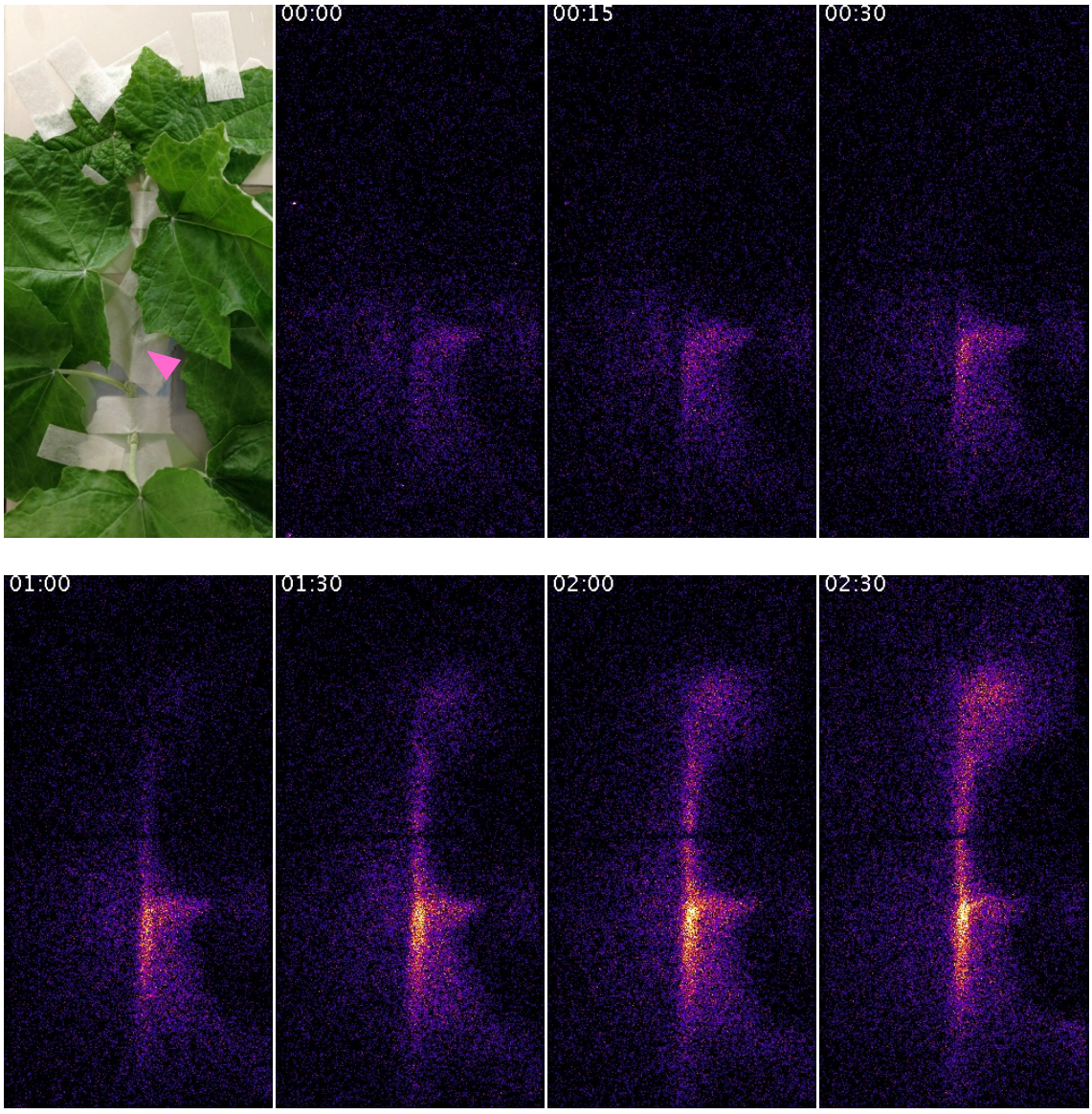


**Fig. 14** Real-time imaging of $^{32}P$ in stage 1. Pink color triangles indicate the position of 6$^{th}$ leaf. The 6$^{th}$ leaf was shielded by acrylic board because its strong signals disturb measurement.

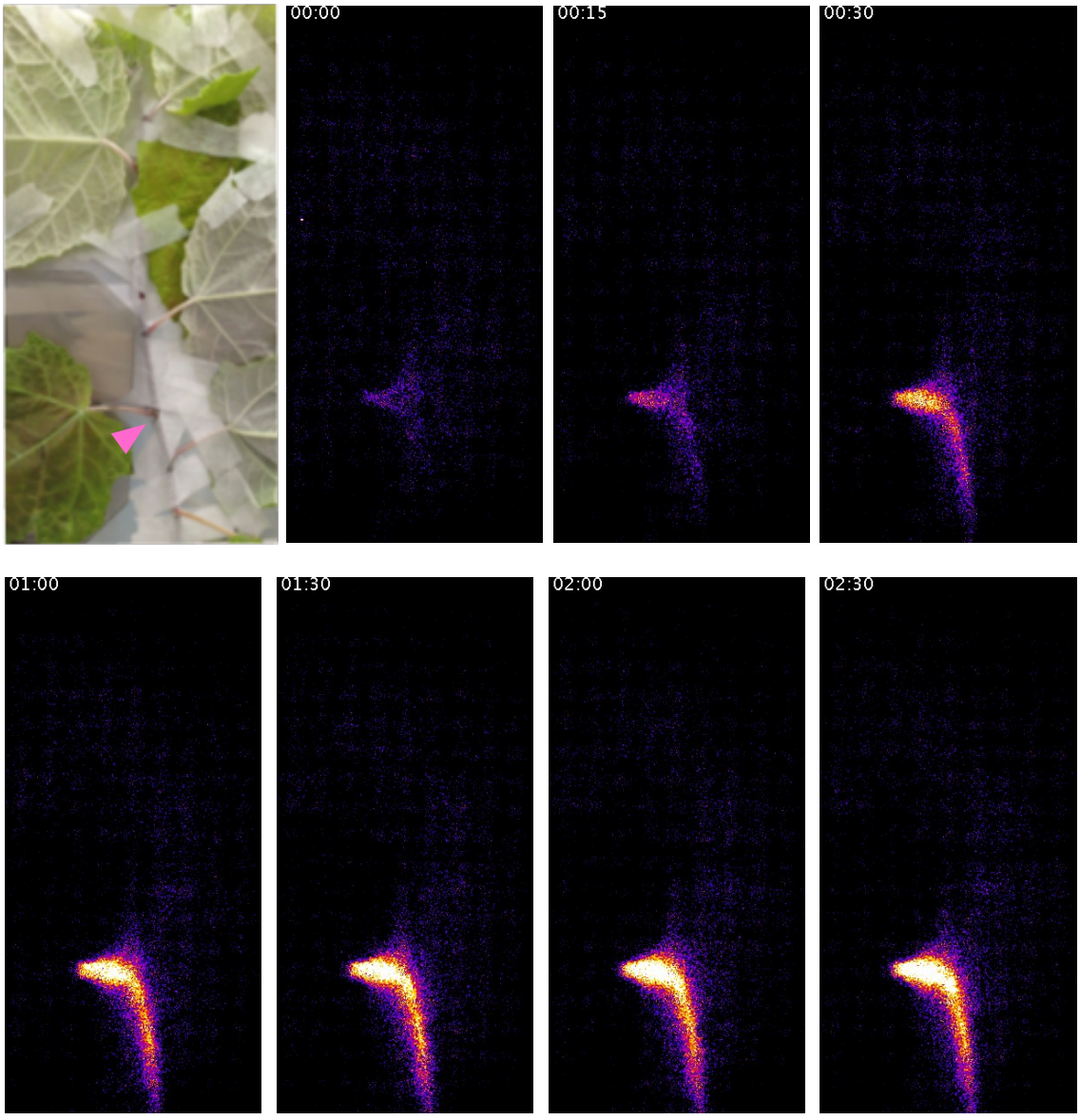


**Fig. 15** Real-time imaging of $^{32}P$ in stage 3. Pink color triangles indicate the position of 6$^{th}$ leaf. The 6$^{th}$ leaf was shielded by acrylic board because its strong signals disturb measurement.

**Interruption of phloem transport and changes in phosphate re-translocation route**

To investigate the contribution of phloem and xylem transport for phosphate re-translocation, interruption of the phloem transport by girdling was performed. When upper bark of the applied leaf was peeled, $^{32}P$ was mainly detected in lower stem and roots after 3 h culture (Fig. 16A). However, after 24 h culture, $^{32}P$ was also detected weakly in upper shoot (Fig. 16A). When lower bark of the applied leaf was peeled, $^{32}P$ was detected in upper shoot after 3 h culture, and higher accumulation of $^{32}P$ in upper shoot was observed even after 24 h culture (Fig. 16B). $^{32}P$ was not detected in lower stem and roots.

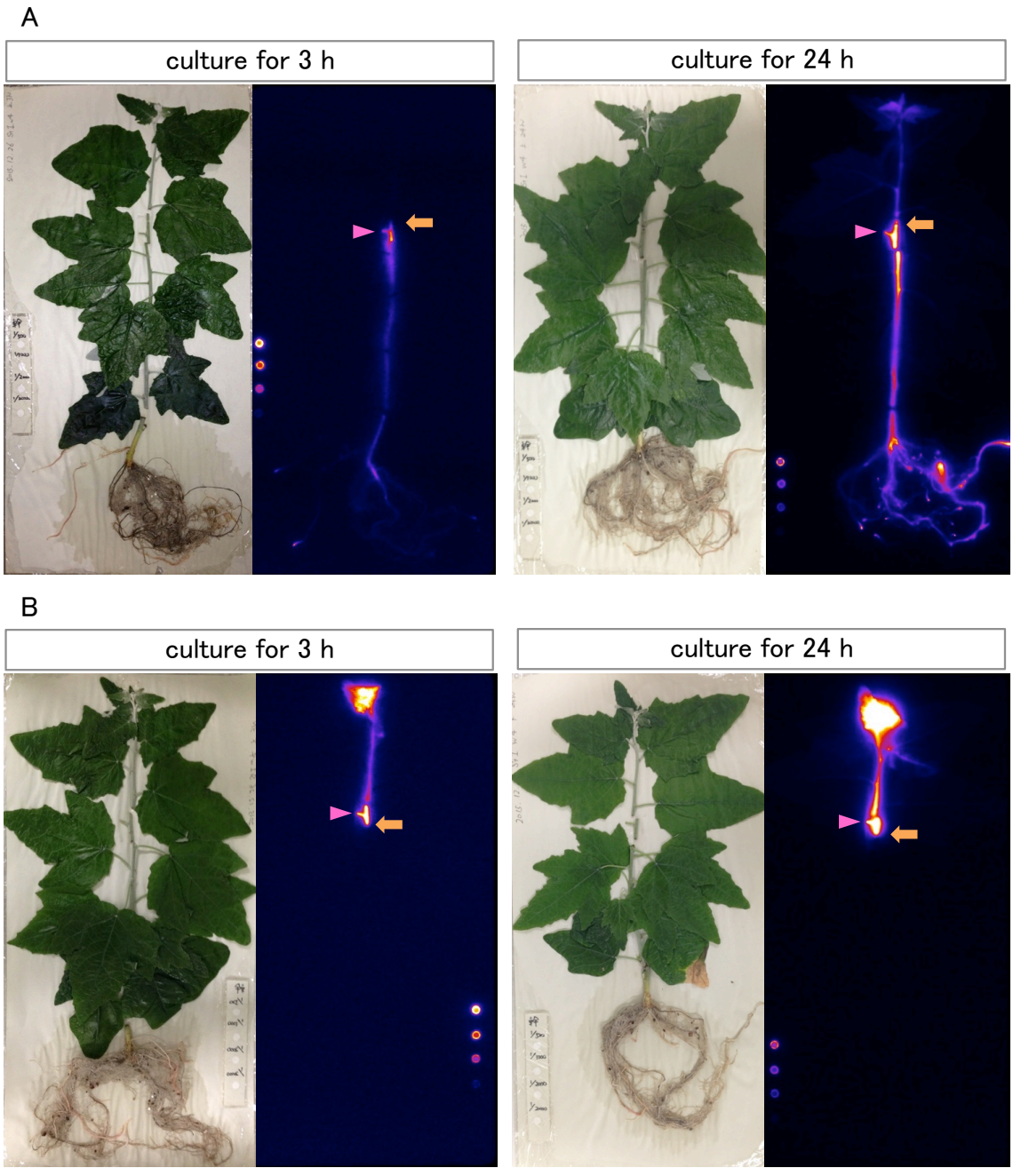


**Fig. 16** Whole plant autoradiographs with phloem girdling. **A** Plants peeled upper bark of 6$^{th}$ leaf were cultured for 3 h or 24 h. **B** Plants peeled lower bark of 6$^{th}$ leaf were cultured for 3 h or 24 h. $^{32}$P solution was added to 6$^{th}$ leaf. After cultivation, upper and lower internodes of 6$^{th}$ leaf were cut to prevent re-translocation of $^{32}$P during contact. **C** The Enlarged view of phloem girdling. Pink color triangles indicate the position of 6$^{th}$ leaf. Orange arrows indicate the position of phloem girdling.

**Seasonal changes in distribution of $^{33}$P at the leaf axil of 6$^{th}$ leaf**

Whole plant autoradiography and real-time imaging revealed seasonal changes in phosphate re-translocation routes and sink tissues (Fig. 13-15). To observe how phosphates flow from the applied leaf to the stem, autoradiography of the leaf axil in stage 1 and 3 was performed (Fig. 17, 18). After 1 day culture from $^{33}$P application to the sixth leaf, sections were obtained, and constructed to 3D images. $^{33}$P from the 6$^{th}$ leaf seemed to flow into the stem through three distinct routes (Fig. 17, 18).

In stage 1, strong signals were detected at the petiole side of phloem of both lower and upper stem, and axial bud (Fig. 17). Weak signals were detected in the whole stem.

In stage 3, strong signals were detected at petiole and phloem of lower stem of the petiole side (Fig. 18). Signals at the upper stem and axial bud were weaker than the lower stem. The distribution of $^{33}$P was detected more in the petiole side, and signals were hardly detected at the opposite side and pith. It should be noted that pith cells are often cracked in this thickness of sections (20 μm), especially samples in stage 3 (Fig. 21). Therefore, $^{33}$P distribution in pith cells could not be clarified in this study.

In stage 3, $^{33}$P was highly detected in petiole, and the zone where a signal is extremely low was observed between the petiole and the stem. It may be a developing abscission layer.

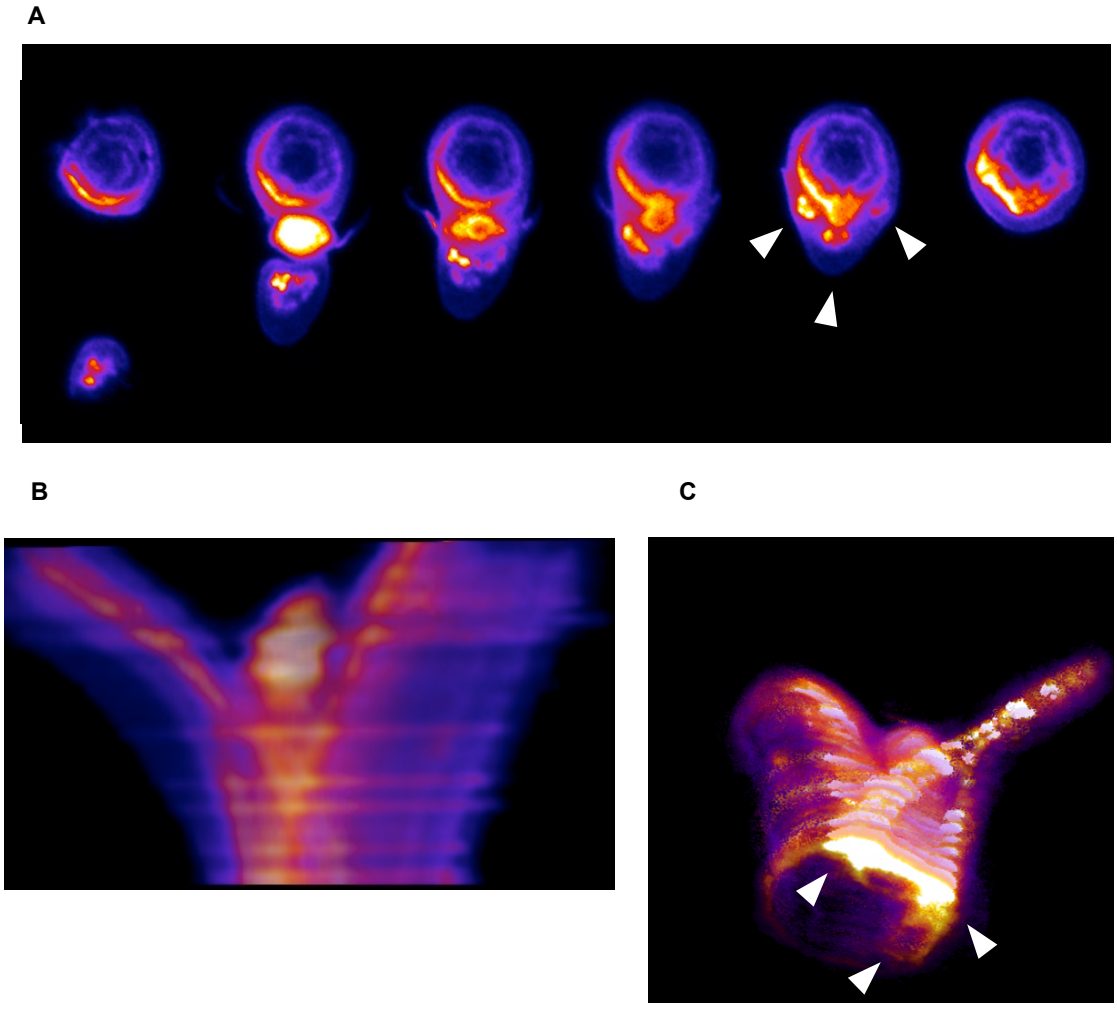


**Fig. 17** $^{33}P$ autoradiographs of leaf axil of 6$^{th}$ leaf in stage 1 using imaging plate. **A** Autoradiographs of leaf axil of 6$^{th}$ leaf . From left to right, sections were placed from upper parts. **B** A side view of the same axil as A. Sections were constructed to 3D images using ImageJ. **C** A view as seen from below of the same axil as A. $^{33}P$ from the 6$^{th}$ leaf seemed to flow into the stem through 3 routes (white triangles).

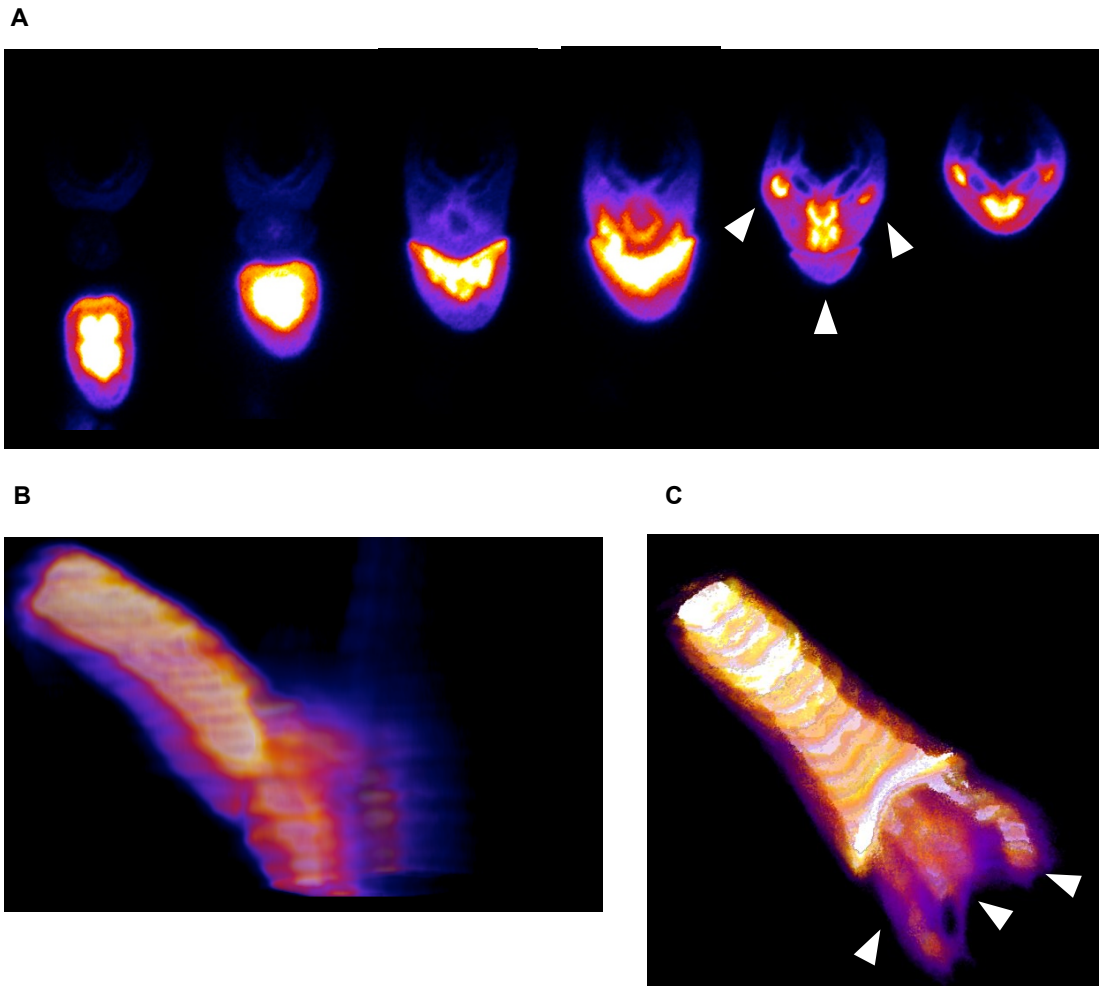


**Fig. 18** $^{33}P$ autoradiographs of leaf axil of 6$^{th}$ leaf in stage 3 using imaging plate. **A** Autoradiographs of leaf axil of 6$^{th}$ leaf . From left to right, sections were placed from upper parts. **B** A side view of the same axil as A. Sections were constructed to 3D images using ImageJ. **C** A view as seen from above of the same axil as A. $^{33}P$ from the 6$^{th}$ leaf seemed to flow into the stem through 3 routes (white triangles).

**Seasonal changes in distribution of $^{33}P$ at the stem of internodes**

To observe seasonal changes in distribution of re-translocated phosphate at the cellular level, $^{33}P$ microautoradiography of the stem between 5$^{th}$ and 6$^{th}$, 6$^{th}$ and 7$^{th}$, 9$^{th}$ and 10$^{th}$ nodes were performed in stage 1 (at 3$^{rd}$ to 4$^{th}$ week) and 3 (at 3$^{rd}$ to 5$^{th}$ week) (Fig. 19-22).

At the stem between 6$^{th}$ and 7$^{th}$ nodes in stage 1, silver particles developed by $^{33}P$ were mainly distributed at the phloem of petiole side (Fig. 19, 20). As well as in Fig.17, silver particles were weakly distributed at the whole section of the stem. In the stem between 5$^{th}$ and 6$^{th}$, or 9$^{th}$ and 10$^{th}$ nodes, two different images of $^{33}P$ distribution were obtained. One was the images that $^{32}P$ was mainly distributed at the phloem of the stem between 5$^{th}$ and 6$^{th}$, and 6$^{th}$ and 7$^{th}$ nodes (Fig. 19). Another was the images that $^{32}P$ was mainly distributed at the phloem of the stem between 5$^{th}$ and 6$^{th}$, and 6$^{th}$ and 7$^{th}$, and 9$^{th}$ and 10$^{th}$ nodes (Fig. 20).

In stage 3, at 3$^{rd}$ to 4$^{th}$ week, silver particles were strongly distributed at phloem, cortex, rays and perimedullary cells in the stem between 6$^{th}$ and 7$^{th}$ nodes (Fig. 21B). Silver particles were obviously observed at the lower level in bast fiber which composed of dead cells. As well as in Fig. 18A, at the opposite side of petiole and pith, silver particles were hardly observed. In the stem between 9$^{th}$ and 10$^{th}$ nodes, silver particles were observed at phloem, and weakly at cortex, ray, perimedullary cell (Fig. 21C). In the stem between 5$^{th}$ and 6$^{th}$ nodes, extremely weaker distribution of silver particles was observed at the petiole side (Fig. 21A).

At 4$^{th}$ to 5$^{th}$ week in stage 3, silver particles were distributed in the similar manner as at 3$^{rd}$ to 4$^{th}$ week, but the density was weaker than that and localization in ray was hardly observed even at the stem between 6$^{th}$ and 7$^{th}$ nodes (Fig. 22).

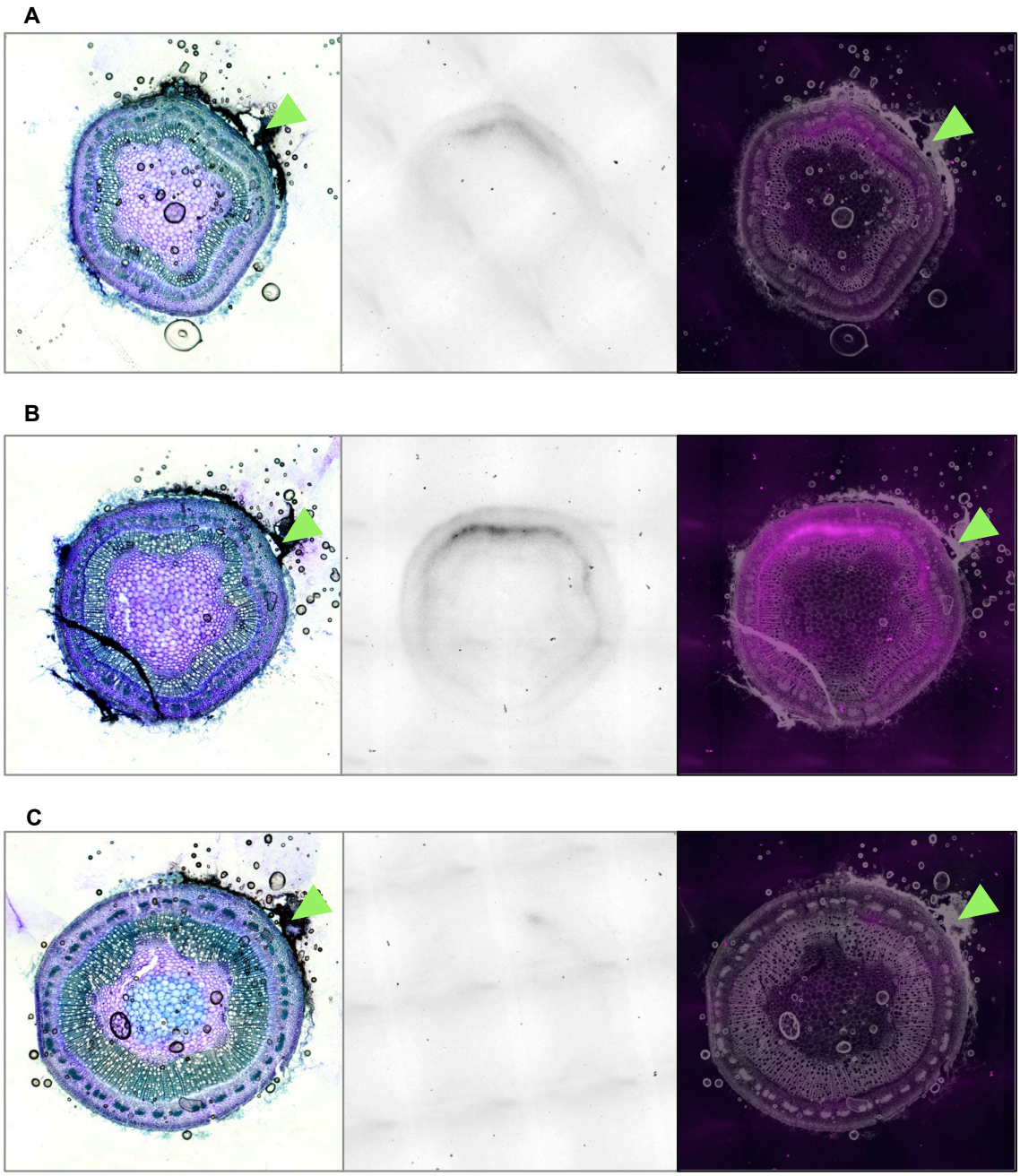


**Fig. 19** Microautoradiographs of the stem in stage 1. **A** the stem between 5th and 6th nodes in stage 1. **B** the stem between 6th and 7th nodes. **C** the stem between 9th and 10th nodes. Left: the stem section stained by toluidine blue. Middle: the microautoradiograph of the section. Right: merged image. Green color triangles indicate the position of 6th leaf.

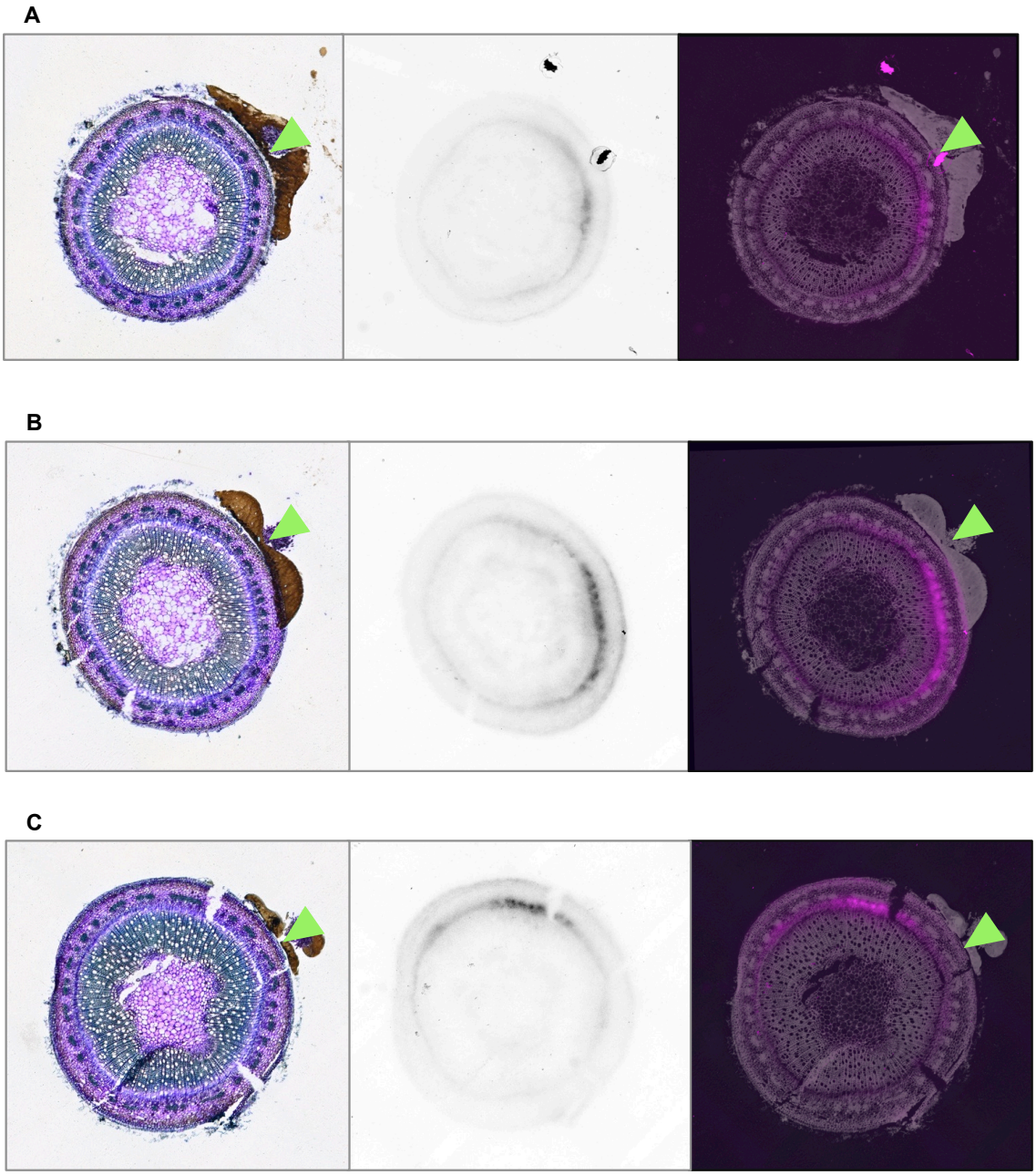


**Fig. 20** Microautoradiographs of the stem in stage 1. **A** the stem between 5$^{th}$ and 6$^{th}$ nodes in stage 1. **B** the stem between 6$^{th}$ and 7$^{th}$ nodes. **C** the stem between 9$^{th}$ and 10$^{th}$ nodes. Left: the stem section stained by toluidine blue. Middle: the microautoradiograph of the section. Right: merged image. Green color triangles indicate the position of 6$^{th}$ leaf.

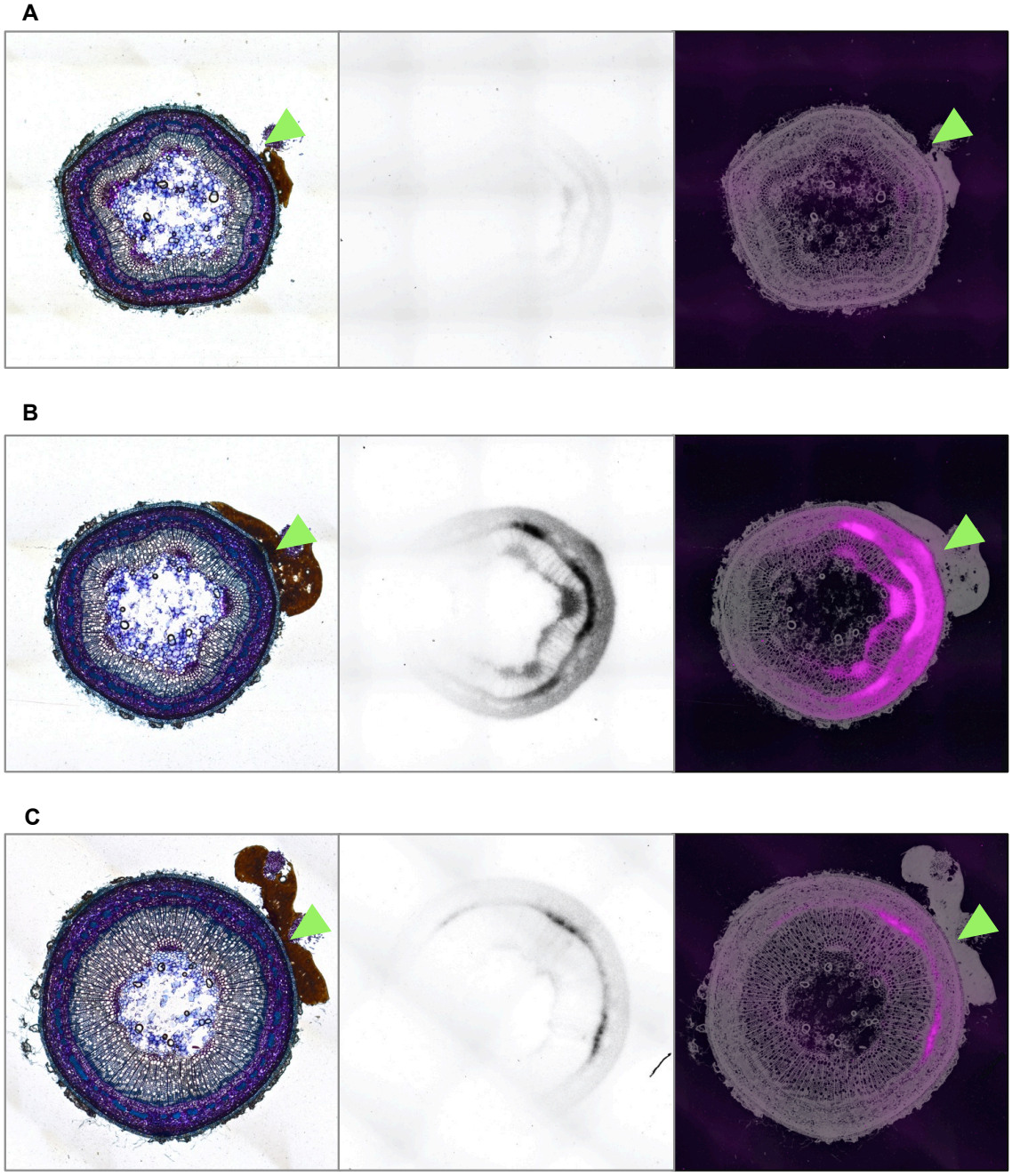


**Fig. 21** Microautoradiographs of the stem at 4th week in stage 3. **A** the stem between 5th and 6th nodes in stage 1. **B** the stem between 6th and 7th nodes. **C** the stem between 9th and 10th nodes. Left: the stem section stained by toluidine blue. Middle: the microautoradiograph of the section. Right: merged image. Green color triangles indicate the position of 6th leaf.

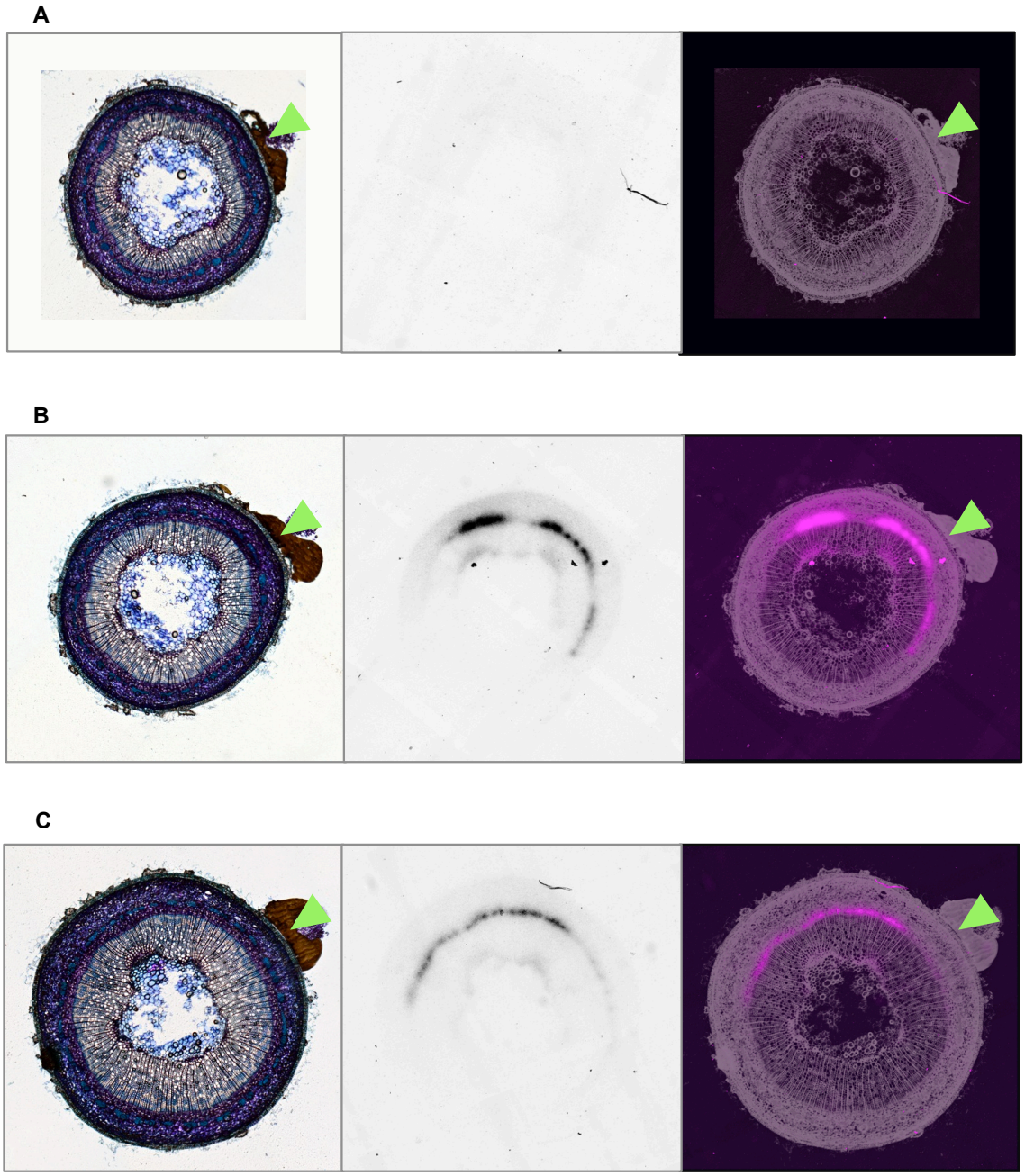


**Fig. 22** Microautoradiographs of the stem at 5th week in stage 3. **A** the stem between 5th and 6th nodes in stage 1. **B** the stem between 6th and 7th nodes. **C** the stem between 9th and 10th nodes. Left: the stem section stained by toluidine blue. Middle: the microautoradiograph of the section. Right: merged image. Green color triangles indicate the position of 6th leaf.

**Direct P re-use from a senescing leaf to new tissues over dormancy in the next spring.**

It was demonstrated that P remobilization from senescing leaves to the storage in perennial tissues occur during dormancy. To confirm contribution of stored P to the leaf expansion in the next spring, whole plant autoradiography over dormancy period was performed in laboratory system. $^{32}P$ was applied to the 6$^{th}$ leaf at 4$^{th}$ week in stage 3. After leaf fall, $^{32}P$ was stored in the stem (Fig. 23). $^{32}P$ was mainly detected in lower stem of the 6$^{th}$ leaf. Then, the same plant was moved to stage 1 and induced bud break. At 4$^{th}$ week in the second stage 1, after development of new shoots, $^{32}P$ was detected in new shoots, roots and stem (Fig. 23). Among them, apices of new leaves and twigs highly accumulated $^{32}P$. Distribution of labeled P was the same at upper and lower side of the 6$^{th}$ leaf.

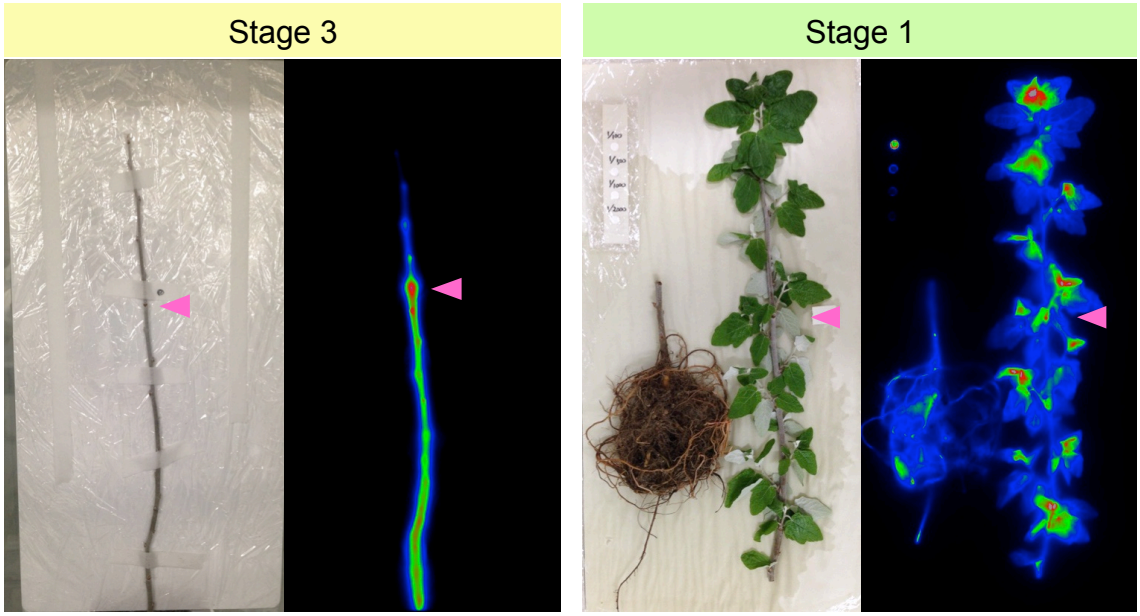


**Fig. 23** Autoradiographs of a whole plant in shortened annual cycle. A plant which applied $^{32}P$ to the 6$^{th}$ leaf in stage 3 was contacted to a imaging plate twice, after leaf fall in stage 3 and after bud burst in next stage 1. Pink color triangles indicate the position of 6$^{th}$ leaf.

**Discussion**

Seasonal changes in re-translocation of phosphate have been investigated by measurement of phosphate contents in leaves or twigs (Chapin and Kedrowski, 1983; Keskitalo et al., 2005; Kurita et al., 2014). However, it was impossible to detect phosphate re-translocation directly by these measurements. In this study, to overcome this difficulty, phosphate re-translocation routes from a mature leaf were visualized by autoradiography using shortened annual cycle.

At the organ level, in stage 1, phosphate was re-translocated to mainly younger leaves and apex from a mature leaf ($6^{th}$ leaf) (Fig. 13). On the other hand, in stage 3, phosphate was re-translocated to the lower stem of the applied leaf. These results indicated seasonal transition of sink tissues and re-translocation route. In stage 1, apical meristem is active and trees grow actively. Then, during stage 2 to 3, trees cease apical growth and leaves start to senesce. Loss of sink ability in apex and younger leaves may lead to the seasonal transition of re-translocation route. In northern red oak, it was observed that C allocation pattern changed with the timing of flushing of new leaves (Dickson, 1989).

Real-time imaging revealed a rapid flow of phosphate in a poplar plant (Fig. 13,14). In stage 1, a poplar could re-translocate phosphate from $6^{th}$ leaf to the apex within one and a half hours (Fig. 14). There seemed to be a time lag between upward and downward flows from applied leaf. The reason of the delay is still unclear. One possibility is a detection threshold of the method. It may not be detected when radioactive P level was too low, even if phosphate was re-translocated. Another possibility is the phloem-xylem exchange. The phloem-xylem exchange about sulfur re-translocation was suggested in previous study, and the girdle did not influence the distribution pattern of the exported $^{35}S$ (Hartmann et al., 2000). Phosphate which

applied to the 6th leaf was re-translocated via phloem. If phosphates from a leaf were transferred from phloem to xylem, and then re-translocated to the apex, such a time lag may occur. However, phloem girdling experiments showed negative evidence to this hypothesis (Fig. 16). Although the exchange from phloem to xylem was observed, P re-translocation to the upper parts was suppressed by phloem girdling, and it suggests that phloem is the main pathway to re-translocate P to upper young tissues in especially short period (3 h). Phloem-xylem exchange and subsequently P re-translocation to the apex via xylem seemed to take more time than direct re-translocation via phloem, at least in the phloem girdling experiments. The 3D image of the 6th leaf axil in stage 1 also showed that the continuous strong $^{32}P$ distribution from petiole to both upper and lower phloem (Fig. 17). Biddulph et al. (1958) reported that $^{32}P$ which applied to a leaf moved through the phloem, and there was little movement from phloem to xylem in red kidney bean. Also, it has been described that phosphorus shows less lateral movement into the xylem than sulphur and carbon-labeled photosynthates (Biddulph, 1956; Biddulph et al., 1958b).

There is another possibility that velocity of the phloem flow to the upper direction is slower or the amount of re-translocated $^{32}P$ is smaller than to the lower direction. In this study, although $^{32}P$ was mainly allocated in apex and young leaves after 1 day culture in stage 1, both whole-plant autoradiography and microautoradiography showed that stronger signals existed in the lower stem under applied leaf than in the upper stem (Fig. 13, 19, 20). These possibilities should be examined by further studies.

In stage 3, phosphate was strongly detected at phloem, rays and perimedullary cells in the lower stem of the applied leaf (Fig. 21B). These distributions of phosphates correspond to the distribution of globoid-like structures in twigs of the field poplar (Fig.

3). It is supposed that phosphates remobilized from senescing leaves were directly accumulated in phloem and xylem parenchyma. The exchange from phloem to xylem probably occur in the stem nearby the applied leaf rather than in the lower stem and roots. Because $^{33}P$ accumulation was stronger in the stem between 6$^{th}$ and 7$^{th}$ nodes than in the stem between 9$^{th}$ and 10$^{th}$ nodes (Fig. 21). Such direct phloem-xylem exchange and storage of P in stem or twigs nearby senescing leaves are reasonable especially in tall trees.

About 1 month later from $^{32}P$ apply, after leaf fall, $^{32}P$ was strongly distributed in lower stem of the applied leaf in stage 3 (Fig. 23). Upward P re-translocation was apparently suppressed during dormancy. This is probably caused by the decreases of transpiration via xylem and upward P re-translocation via phloem (Fig. 18B). From stage 3 to second stage 1, stored $^{32}P$ was re-translocated to the whole plant, not only nearby shoot but also apical shoot.

In shortened annual cycle, sink tissues and routes of re-translocation were shifted by artificial season. How does poplar regulate these transitions? Growth cessation and subsequent leaf senescence probably lead to the loss of sink ability in the apex and young leaves. From stage 2 to 3 (from late summer to winter in field), stem (twigs) started to store $IP_6$ (Fig. 7B, 11C). At 3$^{rd}$ to 4$^{th}$ week in stage 3, $^{32}P$ was strongly accumulated in parenchyma cells in the stem (Fig. 21). Parenchyma cells in perennial tissues have the ability to store nutrients during these seasons. However, at 4$^{rd}$ to 5$^{th}$ week in stage 3, less $^{33}P$ was distributed in parenchyma cells in the stem, and even in the stem between 6$^{th}$ and 7$^{th}$ nodes, silver particles were hardly observed in ray cells (Fig. 22B). This result may indicate the decrease of the storage ability in parenchyma cells and/or the decrease of remobilization by the formation of the abscission layer. However it should be noted that the difficulty to prove the absence of $^{33}P$ by

microautoradiography occurs because the development of silver grains is strongly affected by contact conditions. If the section and the emulsion-coated glass slide are just slightly far placed, silver grains cannot be developed.

In any case, seasonal events, growth cessation, bud set, leaf senescence, nutrient remobilization, storage and the formation of the abscission layer, need to be arranged in an appropriate manner for the efficient nutrient recycling.

**Conclusion and future prospects**

In deciduous tree, although it was well investigated that P is remobilized from senescing leaves, tissues which store P during winter and its storage form have not been clarified until now. Therefore it was unknown how deciduous trees utilize internal P for their long-term survival.

In this study, seasonal P re-translocation was investigated in temperate deciduous woody plant; *Populus alba*. In poplar trees, inorganic and water-soluble organic phosphate was remobilized from senescing leaves during autumn. From late summer to winter, $IP_6$ level strongly increased in twigs. During winter, P was detected at high-electron dense globoid-like structures in protein storage vacuoles in phloem and xylem parenchyma cells in twigs. In early spring, $IP_6$ levels in twigs decreased immediately. These findings suggest that $IP_6$ is the seasonal phosphorus reservoir in the deciduous woody plant, *Populus alba*.

Seasonal P distribution which was revealed by phosphate measurements corresponded to the changes in P re-translocation which was induced by artificial seasons in laboratory. In shortened annual cycle system, radio-labeled P was mainly re-translocated to the apex and young leaves from the he leaf to which $^{32}P$ was applied in growing season (stage 1). During senescing season (stage 3), P was mainly re-translocated to lower stem and roots from the leaf to which $^{32}P$ was applied. In the stem, phloem and xylem parenchyma (like ray) cells is the sink tissues in stage 3. From stage 3 to next stage 1, P which stored in the stem was re-translocated to developing tissues.

Now, It was clarified that the fundamental changes in seasonal P distribution and re-translocation routes in deciduous woody plant; *Populus alba*. How does poplar

tree regulate these mechanisms in all seasons? For the efficient P recycle, P re-translocation to growing tissues, P remobilization from senescing leaves and winter storage and re-translocation in next growing season, must be induced in a proper period. These steps are probably related to other seasonal events, seasonal recycling of other nutrients, growth cessation, bud set, dormancy and its release, etc. It is the next aim to clarify how trees control internal P cycle with other seasonal events and various environmental cues.

## Reference


**Abelson, P.H.** (1999). A potential phosphate crisis. Science **283**: 2015.

**Aerts, R.** (1996). Nutrient resorption from senescing leaves of perennials: are there general patterns? J. Ecol. **84**: 597–608.

**Biddulph, O., Biddulph, S., Cory, R., and Koontz, H.** (1958a). Circulation Patterns for Phosphorus, Sulfur and Calcium in the Bean Plant. Plant Physiol. **33**: 293–300.

**Biddulph, S., Biddulph, O., and Cory, R.** (1958b). Visual Indications of Upward Movement of Foliar-Applied $P^{32}$ and $C^{14}$ in the Phloem of the Bean Stem. America (NY). **45**: 648–652.

**Biddulph, S.F.** (1956). Visual Indication of $S^{35}$ and $P^{32}$ Translocation in the Phloem. America (NY). **43**: 143–148.

**Böhlenius, H., Huang, T., Charbonnel-Campaa, L., Brunner, A.M., Jansson, S., Strauss, S.H., and Nilsson, O.** (2006). CO/FT regulatory module controls timing of flowering and seasonal growth cessation in trees. Science **312**: 1040–1043.

**Bücking, H. and Heyser, W.** (2001). Microautoradiographic localization of phosphate and carbohydrates in mycorrhizal roots of *Populus tremula* x *Populus alba* and the implications for transfer processes in ectomycorrhizal associations. Tree Physiol. **21**: 101–107.

**Chapin, F.S. and Kedrowski, R.A.** (1983). Seasonal Changes in Nitrogen and Phosphorus Fractions and Autumn Retranslocation in Evergreen and Deciduous Taiga Trees. Ecology **64**: 376–391.

**Cherbuy, B., Joffre, R., Gillon, D., and Rambal, S.** (2001). Internal remobilization of carbohydrates, lipids, nitrogen and phosphorus in the Mediterranean evergreen oak *Quercus ilex*. Tree Physiol. **21**: 9–17.

**Chiou, T.-J., Aung, K., Lin, S.-I., Wu, C.-C., Chiang, S., and Su, C.-L.** (2006). Regulation of Phosphate Homeostasis by MicroRNA in Arabidopsis. Plant Cell **18**: 412–421.

**Cooke, J.E.K., Eriksson, M.E., and Junttila, O.** (2012). The dynamic nature of bud dormancy in trees: Environmental control and molecular mechanisms. Plant, Cell Environ. **35**: 1707–1728.

**Dickson, R.E.** (1989). Carbon and nitrogen allocation in trees. Transport **46**: 631s–647s.

**Dickson, R.E., Vogelmann, T.C., and Larson, P.R.** (1985). Glutamine Transfer from Xylem to Phloem and Translocation to Developing Leaves of *Populus deltoides*. Plant Physiol. **77**: 412–417.

**Fracheboud, Y., Luquez, V., Björkén, L., Sjödin, A., Tuominen, H., and Jansson, S.** (2009). The control of autumn senescence in European aspen. Plant Physiol. **149**: 1982–1991.

**Fujii, H., Chiou, T.-J., Lin, S.-I., Aung, K., and Zhu, J.K.** (2005). A miRNA involved in phosphate-starvation response in Arabidopsis. Curr. Biol. **15**: 2038–2043.

**Hadi Alkarawi, H. and Zotz, G.** (2014). Phytic acid in green leaves. Plant Biol. **16**: 697–701.

**Hartmann, T., Mult, S., Suter, M., Rennenberg, H., and Herschbach, C.** (2000). Leaf age-dependent differences in sulphur assimilation and allocation in poplar (*Populus tremula* x *P. alba*) leaves. J. Exp. Bot. **51**: 1077–1088.

**Hatch, A.J. and York, J.D.** (2010). SnapShot : Inositol Phosphates. Cell **143**: 1030–1031.

**Herschbach, C., Gessler, A., and Rennenberg, H.** (2012). Long-distance transport and plant internal cycling of N- and S-compounds. Prog. Bot. **73**: 161–188.

**Herschbach, C. and Rennenberg, H.** (1996). Storage and remobilisation of sulphur in beech trees (*Fagus sylvatica*). Physiol. Plant. **98**: 125–132.

**Hirose, A., Kobayashi, N.I., Tanoi, K., and Nakanishi, T.M.** (2014). A Microautoradiographic Method for Fresh-Frozen Sections to Reveal the Distribution of Radionuclides at the Cellular Level in Plants. Plant Cell Physiol. **55**: 1194–1202.

**Hirose, A., Yamawaki, M., Kanno, S., Igarashi, S., Sugita, R., Ohmae, Y., Tanoi, K., and Nakanishi, T.M.** (2013). Development of a $^{14}C$ detectable real-time radioisotope imaging system for plants under intermittent light environment. J. Radioanal. Nucl. Chem. **296**: 417–422.

**Horvath, D.** (2009). Common mechanisms regulate flowering and dormancy. Plant Sci. **177**: 523–531.

**Kanno, S., Yamawaki, M., Ishibashi, H., Kobayashi, N.I., Hirose, A., Tanoi, K., Nussaume, L., and Nakanishi, T.M.** (2012). Development of real-time radioisotope imaging systems for plant nutrient uptake studies. Philos. Trans. R. Soc. B Biol. Sci. **367**: 1501–1508.

**Kawamoto, T.** (2003). Use of a new adhesive film for the preparation of multi-purpose fresh-frozen sections from hard tissues, whole-animals, insects and plants. Arch. Histol. Cytol. **66**: 123–143.

**Keskitalo, J., Bergquist, G., Gardenström, P., and Jansson, S.** (2005). A Cellular Timetable of Autumn Senescence. Plant Physiol. **139**: 1635–1648.

**Kobayashi, N.I., Tanoi, K., Hirose, A., and Nakanishi, T.M.** (2013). Characterization of rapid intervascular transport of cadmium in rice stem by radioisotope imaging. J. Exp. Bot. **64**: 507–517.

**Kurita, Y., Baba, K., Ohnishi, M., Anegawa, A., Shichijo, C., Kosuge, K., Fukaki, H., and Mimura, T.** (2014). Establishment of a shortened annual cycle system ; a tool for the analysis of annual re-translocation of phosphorus in the deciduous woody plant ( *Populus alba* L .). J. Plant Res. **127**: 545–551.

**Lin, W.Y., Lin, S.I., and Chiou, T.-J.** (2009). Molecular regulators of phosphate homeostasis in plants. J. Exp. Bot. **60**: 1427–1438.

**Loth-Pereda, V., Orsini, E., Courty, P.E., Lota, F., Kohler, A., Diss, L., Blaudez, D., Chalot, M., Nehls, U., Bucher, M., and Martin, F.** (2011). Structure and Expression Profile of the Phosphate Pht1 Transporter Gene Family in Mycorrhizal Populus trichocarpa. Plant Physiol. **156**: 2141–2154.

**Lott, J.N.A., Ockenden, I., Raboy, V., and Batten, G.D.** (2000). Phytic acid and phosphorus in crop seeds and fruits: a global estimate. Seed Sci. Res. **10**: 11–33.

**Mimura, T.** (1995). Homeostasis and transport of inorganic phosphate in plants. Plant Cell Physiol. **36**: 1–7.

**Mimura, T., Sakano, K., and Shimmen, T.** (1996). Studies on the distribution , re-transiocation and homeostasis of inorganic phosphate in barley leaves. Plant, Cell Environ. **19**: 311–320.

**Mitsuhashi, N., Ohnishi, M., Sekiguchi, Y., Kwon, Y.-U., Chang, Y.-T., Chung, S.-K., Inoue, Y., Reid, R.J., Yagisawa, H., and Mimura, T.** (2005). Phytic Acid Synthesis and Vacuolar

Accumulation in Suspension-Cultured Cells of Catharanthus roseus Induced by High Concentration of Inorganic. Plant Physiol. **138**: 1607–1614.

**Murphy, J. and Riley, J.P.** (1962). A modified single solution method for the determination of phosphate in natural waters. Anal. Chim. Acta **27**: 31–36.

**Otegui, M.S., Capp, R., and Staehelin, L.A.** (2002). Developing seeds of Arabidopsis store different minerals in two types of vacuoles and in the endoplasmic reticulum. Plant Cell **14**: 1311–1327.

**Preibisch, S., Saalfeld, S., and Tomancak, P.** (2009). Globally optimal stitching of tiled 3D microscopic image acquisitions. Bioinformatics **25**: 1463–1465.

**Raboy, V.** (2003). myo-Inositol-1,2,3,4,5,6-hexakisphosphate. Phytochemistry **64**: 1033–1043.

**Ravindran, V., Ravindran, G., and Sivalogan, S.** (1994). Total and phytate phosphorus contents of various foods and feedstuffs of plant origin. Food Chem. **50**: 133–136.

**Rennenberg, H. and Herschbach, C.** (2013). Phosphorus nutrition of woody plants: many questions - few answers. Plant Biol. **15**: 785–788.

**Rohde, A., Bastien, C., and Boerjan, W.** (2011). Temperature signals contribute to the timing of photoperiodic growth cessation and bud set in poplar. Tree Physiol. **31**: 472–482.

**Rohde, A. and Bhalerao, R.P.** (2007). Plant dormancy in the perennial context. Trends Plant Sci. **12**: 217–223.

**Salisbury, F.B. and Ross, C.W.** (1992). Plant physiology. In (Wadsworth: Belmont, CA.).

**Samotus, B. and Schwimmer, S.** (1962). Phytic acid as a phosphorus reservoir in the developing potato tuber. Nature **194**: 578 – 579.

**Sauter, J.J. and van Cleve, B.** (1994). Storage, mobilization and interrelations of starch, sugars, protein and fat in the ray storage tissue of poplar trees. Trees **8**: 297–304.

**De Schepper, V., De Swaef, T., Bauweraerts, I., and Steppe, K.** (2013). Phloem transport: A review of mechanisms and controls. J. Exp. Bot. **64**: 4839–4850.

**Sheard, L.B. et al.** (2010). Jasmonate perception by inositol-phosphate-potentiated COI1-JAZ co-receptor. Nature **468**: 400–405.

**Shim, D., Ko, J.H., Kim, W.C., Wang, Q., Keathley, D.E., and Han, K.H.** (2014). A molecular framework for seasonal growth-dormancy regulation in perennial plants. Hortic. Res. **1**: 14059.

**Sugita, R., Kobayashi, N.I., Hirose, A., Ohmae, Y., Tanoi, K., and Nakanishi, T.M.** (2013). Nondestructive real-time radioisotope imaging system for visualizing $^{14}$C-labeled chemicals supplied as CO<sub>2 in plants using Arabidopsis thaliana. J. Radioanal. Nucl. Chem. **298**: 1411–1416.

**Sweetman, D., Johnson, S., Caddick, S.E.K., Hanke, D.E., and Brearley, C. a** (2006). Characterization of an *Arabidopsis* inositol 1,3,4,5,6-pentakisphosphate 2-kinase (AtIPK1). Biochem. J. **394**: 95–103.

**Tan, X., Calderon-Villalobos, L.I.A., Sharon, M., Zheng, C., Robinson, C. V, Estelle, M., and Zheng, N.** (2007). Mechanism of auxin perception by the TIR1 ubiquitin ligase. Nature **446**: 640–645.

**Turner, B.L., Papházy, M.J., Haygarth, P.M., and McKelvie, I.D.** (2002). Inositol phosphates in the

environment. Philos. Trans. R. Soc. Lond. B. Biol. Sci. **357**: 449–469.

**Windt, C.W., Vergeldt, F.J., De Jager, P.A., and Van As, H.** (2006). MRI of long-distance water transport: A comparison of the phloem and xylem flow characteristics and dynamics in poplar, castor bean, tomato and tobacco. Plant, Cell Environ. **29**: 1715–1729.

**El Zein, R., Bréda, N., Gérant, D., Zeller, B., and Maillard, P.** (2011). Nitrogen sources for current-year shoot growth in 50-year-old sessile oak trees: An in situ $^{15}N$ labeling approach. Tree Physiol. **31**: 1390–1400.

**Zhu, B. and Coleman, G.D.** (2001). Phytochrome-mediated photoperiod perception, shoot growth, glutamine, calcium, and protein phosphorylation influence the activity of the poplar bark storage protein gene promoter (bspA). Plant Physiol. **126**: 342–351.

**Acknowledgements**

First of all, I would like to sincerely thank Dr. Kei'ichi Baba for monthly sampling and teaching electron micrographs and gracious answers and discussions to my questions.

■About chapter 1;

I would like to offer my heartfelt thanks to Dr. Toshinobu Suzaki, Dr. Park Pyoyun and Dr. Megumi Matsumoto for their precious advice and Technical guidance about Electron microscopy and EDXS, to Dr. Keiko Kosuge for her support about sampling of various trees and advice about the botany of trees, and to Dr. Yoko Sekiguchi and Ms. Kimiko Fujisawa for their kind supports to $IP_6$ measurement.

■About chapter 2;

I'm deeply grateful to Dr. Shinobu Satoh for his advice about culture conditions for the establishment of a shortened annual cycle.

■About chapter 3;

I greatly appreciate to Dr. Tomoko M. Nakanishi, Dr. Keitaro Tanoi, Dr. Atsushi Hirose, Dr. Ryohei Sugita and Dr. Satomi Kanno for their guidance and precious advice about MAR and RRIS. Especially, Atsushi Hirose, Dr. Ryohei Sugita and Dr. Satomi Kanno gave me their precious time for experiments and analysis very much.

I also greatly appreciate to Dr. Tatsuaki Goh for his guidance about imageJ.

I greatly appreciate to my thesis advisor, Dr. Hiroshi Kawai, Dr. Keiko Kosuge, Dr. Hidehiro Fukaki, and apologize for the delay in submission of draft.

I'm deeply grateful to Dr. Hidehiro Fukaki, Dr. Chizuko Shichijo, Dr. Kimitsune Ishizaki, Dr. Miwa Ohnishi, Dr. Aya Anegawa, Dr. Tatsuaki Goh, Dr. Koichi Toyokura, and members of Mimura, Fukaki, Shichijo and Ishizaki's laboratory for their kind discussion and incisive comments and many helps.

From the bottom of my heart, I really appreciate Dr. Tetsuro Mimura granting my request that I want to study about trees and giving this very interesting research theme, and supporting daily in laboratory. I'm very glad to find the thing that can continue challenging without getting tired.

Finally, I would like to thank you all again, and thank poplar trees that keep enduring constant disaster in the name of science.